QC
880
.A4
no.
76/11

ERL-ATDL-76/11

06295

# Environmental Research Laboratories

## Air Resources
## Atmospheric Turbulence and Diffusion Laboratory

## Oak Ridge, Tennessee

ETAC/CBT
FILE COPY
30 JAN 1977

JULY 1976

# FIRST ANNUAL REPORT ON WEATHER MODIFICATION EFFECTS OF COOLING TOWERS

S. R. Hanna
R. P. Hosker, Jr.

ATDL Contribution File No. 76/11

U. S. DEPARTMENT OF COMMERCE
NATIONAL OCEANIC AND ATMOSPHERIC ADMINISTRATION

QC
880
.A4
no.76/11

# FIRST ANNUAL REPORT
# ON
# WEATHER MODIFICATION EFFECTS OF COOLING TOWERS

to
U. S. Environmental Protection Agency
and
U. S. Energy Research and Development Administration

from
National Oceanic and Atmospheric Administration
Air Resources Atmospheric Turbulence and Diffusion Laboratory
Oak Ridge, Tennessee

LIBRARY
SEP 29 2015
National Oceanic &
Atmospheric Administration
U.S. Dept. of Commerce

#38275885

S. R. Hanna
R. P. Hosker, Jr.

28 JAN 1998

July, 1976
ATDL Contribution File No. 76/11

TABLE OF CONTENTS




AWS TECHNICAL LIBRARY
FL 4414
859 BUCHANAN STREET
SCOTT AFB IL 62225-5118

# CHAPTER I

## INTRODUCTION AND SUMMARY

This is the first annual report on work accomplished at the National Oceanic and Atmospheric Administration's Air Resources Atmospheric Turbulence and Diffusion Laboratory (ATDL), Oak Ridge, Tennessee, on "Weather Modification Effects of Cooling Towers." This research was carried out under an interagency agreement between the U. S. Environmental Protection Agency and the U. S. Energy Research and Development Administration under the general title "Cooling System Program," Interagency Energy Accomplishment Plan I. D. no. 77BCD, IAG I.D. no. D5-E681, program element EHA541, Task no. T/A 1.b, dated April 16, 1975. The principal investigator is F. A. Gifford, Jr., Director of ATDL. Participating ATDL scientists include G. A. Briggs, S. R. Hanna, R. P. Hosker, Jr., and K. S. Rao.

Chapter II reports on a cooling tower plume and cloud growth model developed at ATDL by S. R. Hanna. Using observed atmospheric vertical profiles of temperature, dew point and wind speed, and the source parameters for a cooling tower, the ATDL plume and cloud growth model estimates the variation with height of vertical speed, temperature, water vapor content, and liquid water content in the plume. The present model is one dimensional and steady state, but

future plans call for the development of multidimensional models. The model predictions are compared to observations of cooling tower plumes at the Rancho Seco and John E. Amos power plants and a refinery cloud. Fair agreement is obtained between estimates and observations of excess water and temperature in the plume, visible plume length, and plume rise. The model is also applied to 241 radiosonde soundings from Nashville, using four hypothetical sources ranging from a single 1000 MW cooling tower to a $10^5$ MW power park. It is estimated that liquid water will form at the top of the plume 39% of the time for the $10^3$ MW tower. Estimated visible plume length and plume rise are presently being compared with observations from TVA's Paradise, Kentucky, cooling tower.

Chapter III presents the plans for laboratory study of flow and plume behavior near single and multiple cooling towers of different types. An extensive survey of the laboratory simulation literature has been completed, requirements for the requisite modeling facility formulated, and equipment, including a suitable wind tunnel, purchased. Funding and construction delays in obtaining a building to house the tunnel have unavoidably postponed the start of the experimental test program. It is presently anticipated that the finished facility will be in operation before January 1, 1977, roughly six months behind the original schedule.

Chapter IV provides a new tentative schedule of accomplishment. An accelerated laboratory test program should permit meeting the original project deadline for completion with no serious difficulty.

Chapter V lists the references cited in the theoretical and experimental sections.

CHAPTER II

# DEVELOPMENT AND APPLICATIONS OF A COOLING TOWER PLUME AND CLOUD GROWTH MODEL

by
Steven R. Hanna

## 1. Introduction

Single cooling towers emit as much as 1000 MW of sensible and latent heat to the atmosphere. Planned energy centers or power parks may contain clusters of cooling towers which emit a total of 100,000 MW. As shown by Hanna and Gifford (1975) heat releases of this magnitude have the potential to significantly alter local weather. Cooling towers can also alter the local environment by the production of fog and clouds, and the deposition of drift salts.

There are several models available for estimating drift deposition and visible plume length from single cooling towers (see Cooling Tower Environment - 1974 and McVehil and Heikes, 1975). However, there are no data suitable for testing the drift deposition models and very few data suitable for testing the visible plume models. Currently a drift deposition experiment is underway at Chalk Point, Maryland, (Environmental Systems Corporation, 1976) as part of a comprehensive study of the salt water natural draft cooling tower at that site. A few measurements of visible plume length are available (e.g.; Slawson et al., 1974; Meyer et al., 1974), and there are several more sets of measurements that are just being published. Three of the new sets of visible plume observations

are compared with model predictions in this report. These are the observations of cooling tower plumes at the John E. Amos fossil power plant (Kramer et al., 1975), the Rancho Seco nuclear power plant (Wolf, 1976), and a refinery plume near St. Louis (Auer, 1976).

The basic model presented in this report is a simple one-dimensional model (variables are functions only of height). Since the cooling tower emissions are usually constant with time, at least over time periods less than four or five hours, the steady-state assumption is good. Phenomena such as multiple plume merging and changes in the environmental air surrounding the plume are accounted for only by crude parameterization. According to our plan, this model is only the first in a series of models, and future models will be multidimensional and able to handle plume-environment interactions. Other members of our research group, S. Rao and C. Nappo (1976), are developing second order closure and fully turbulent models of multiple plumes.

A thorough description of the one-dimensional numerical model for plume and cloud growth that is used in the analyses in later sections is given in Section 2 of the paper by Hanna (1976a), to be published in Atmospheric Environment, appended to this report(Appendix A). Section 3 of Appendix A describes the input data that are necessary to run the model.

2. John E. Amos Cooling Towers

During the winter of 1974-1975, Smith-Singer Meteorologists, Inc. obtained measurements with a light aircraft around the three cooling tower plumes at the John E. Amos power plant in West Virginia (Kramer et al., 1975). Experiments were performed only on cold, humid mornings when long visible plumes were expected. The aircraft measured vertical profiles of temperature and dew point, and roughly estimated the wind speed. Photographs of the visible plume were taken, but the aircraft did not penetrate the plume. Plant personnel provided data on the load of the cooling towers.

The plant ran close to its rated capacity of 2900 MW during most of the experiments. In the model, the plume from a single tower is followed until its radius, R, equals one half of the distance, s, between the towers (s=200m). The initial plume radius, $R_o$, and vertical speed, $w_o$, equal 40m and 4.4m/s, respectively. To insure continuity of the momentum flux, the effective initial plume radius for bent-over plumes is calculated from the equation (Hanna, 1972):

$$R_{eff} = R_o(w_o/U)^{1/2}, \qquad (1)$$

where U is the wind speed. Using the specifications given by Kramer et al (1975), the initial plume temperature, $T_{po}$, at full load is assumed to be given by the relation:

$$T_{po} = (297.4 + .635(T_d - 273))(1 + .01(1-RH)), \qquad (2)$$

where $T_d$ is the ambient dew point and RH is the ambient relative humidity. For power outputs less than full load, initial plume temperature is calculated from:

$$\frac{T_{po} - T_{eo}}{T_{po}(\text{eq.2}) - T_{eo}} = \frac{\text{actual load}}{2900 \text{ mw}} \quad , \qquad (3)$$

where $T_{eo}$ is the ambient temperature. Initial plume cloud water, $Q_c$, and hydrometeor water, $Q_H$, are arbitrarily set equal to .001 g/g, on the basis that fog or cloud is obviously present at the tower mouth. This estimate could be made more accurate if observations of liquid water at the tower mouth were taken.

About half of the sets of observations could not be used because of uncertainties in the temperature profiles or plume photographs. Of the 27 sets that were used, the input data for four are given in Appendices A and B (Hanna, 1976a and 1976b). Kramer et al. (1975) give complete listings of all the data.

## 2.1 Plume Rise at Amos

In 19 of the runs studied, the observed visible plume passed through the point of maximum plume rise. A comparison of observed and predicted plume rise is given in Table 1, showing that the average predicted plume rise (670m) is close to the average observed rise (750m). The correlation coefficient is 0.49, which is only fair. The last column of the table contains Briggs (1975) analytical plume rise prediction, where the initial buoyancy flux is assumed to equal the sensible heat flux from the largest tower. The average predicted rise is 540m and the correlation with observations is 0.37. Column five in the table contains the observed height of the base of the capping inversion or mixing layer, which is seen to be well-correlated (0.90) with the observed plume rise. Brennan et al, (1976) have analyzed these data and find that when a capping inversion is present the plume will level off after striking it. This rule is probably not valid in the summer when the height of the capping inversion is much higher and the plume is likely to reach final rise before striking the inversion.

Some examples of predicted vertical profiles of $Q_c$, w, and $(T_p-T_e)$ are given in Figures 1-3 of Appendix B. The predicted cloud water content, $Q_c$, is generally about .5 to 1.5 g/kg, which agrees with observations in natural cumulus clouds. The maximum vertical speed,

Table 1

Observed and Calculated Plume Rise at John E. Amos Power Plant

| Run | $\bar{U}$ (m/s) | Ambient tower top saturation deficit (g/kg) | $\Delta\theta/\Delta Z$ over depth of plume ($°C/m \times 10^3$) | Inversion height above tower (m) | Observed plume rise (m) | Model plume rise (m) | Analytical plume rise sensible one unit (m) |
|---|---|---|---|---|---|---|---|
| 1 | 14 | .43 | 13.5 | | 560 | 260 | 250 |
| 6 | 11 | .13 | 3.0 | | 850 | 820 | 430 |
| 8a | 9 | 0 | 9.8 | | 370 | 350 | 250 |
| 10a | 5 | .60 | 2.1 | 720 | 820 | 820 | 590 |
| 11 | 0 | 1.34 | 6.1 | 660 | 880 | 900 | 980 |
| 12 | 6 | 1.25 | 1.2 | 1140 | 1060 | 1200 | 720 |
| 15 | 3 | .28 | 10.7 | | 1120 | 790 | 780 |
| 16 | 6 | .41 | 7.2 | 1200 | 1160 | 700 | 380 |
| 17a | 8 | .29 | 6.7 | 360 | 360 | 430 | 410 |
| 18 | 6 | .78 | 5.6 | | 910 | 720 | 410 |
| 19 | 0 | 1.07 | 6.9 | 840 | 800 | 970 | 910 |
| 24 | 6 | .60 | 4.0 | 750 | 760 | 630 | 500 |
| 28a | 5 | .52 | 21.8 | | 360 | 400 | 310 |
| 31 | 0 | 1.02 | 11.6 | | 500 | 900 | 780 |
| 35a | 3 | .87 | 9.8 | 390 | 360 | 590 | 480 |
| 44 | 8 | 1.16 | 1.9 | 960 | 910 | 420 | 510 |
| 45 | 7 | 1.16 | 5.6 | 1200 | 910 | 370 | 390 |
| 47 | 0 | 1.44 | 3.8 | 900 | 800 | 1020 | 910 |
| 48a | 7 | 1.46 | 7.6 | 750 | 670 | 360 | 340 |
| Avg. | 5.6 | .76 | 7.4 | 820 | 750 | 670 | 540 |

w, is between 4 and 10 m/s. The temperature excess, $(T_p-T_e)$ is seen to decrease almost linearly with log z for the runs plotted. Unfortunately there were no in-plume measurements during this experiment that could be used to test these predictions.

2.2 Visible Plume Length at Amos

There are seven runs in which the visible plume is moderately long but does not reach the point of maximum plume rise. These runs are summarized in Table 2. The results of a simple analytical model (Hanna, 1974) are also given, where it is assumed that the tip of the visible plume occurs when the initial flux of excess water, $w_o R_o^2 Q_{po}$, in the plume equals the saturation deficit flux, $UR^2(Q_{eos}-Q_{eo})$:

$$h = 2R_o(w_o/U)^{1/2}[(2Q_{po}/(Q_{eos}-Q_{eo}))^{1/2}-1] \qquad (4)$$

$$\ell = 1.4(R_o^{3/2}U^{3/4}w_o^{3/4}/F^{1/2})[(2Q_{po}/(Q_{eos}-Q_{eo}))^{1/2}-1]^{3/2} \qquad (5)$$

In these equations h is visible plume height, $\ell$ is visible plume length, subscripts p, e, o, and s refer to plume, environmental, initial, and saturated variables, respectively, and F is the initial buoyancy flux:

$$F = (g/T_{po})w_o R_o^2 (T_{po}-T_{eo}) \qquad (6)$$

Table 2

Visible Plume Dimensions for Plumes whose Visible Portion does not Reach the Point of Maximum Rise, for John E. Amos Power Plant

| Run | $\bar{U}$ (m/s) | ambient saturation deficit (g/Kg) | | observed | | numerical model | | analytical model | | ambient RH at plume level |
|---|---|---|---|---|---|---|---|---|---|---|
| | | tower top | plume level | visible plume height (m) | visible plume length (m) | visible plume height (m) | visible plume length (m) | visible plume height (m) | visible plume length (m) | |
| 2 | 13 | 3.0 | 3.9 | 100 | 200 | 75 | 290 | 100 | 370 | .4 |
| 3 | 10 | 2.6 | 2.7 | 150 | 500 | 120 | 350 | 140 | 400 | .65 |
| 13 | 10 | .86 | 1.8 | 100 | 300 | 150 | 480 | 210 | 730 | .6 |
| 20 | 10 | 2.8 | 3.9 | 200 | 400 | 70 | 250 | 120 | 290 | .45 |
| 27 | 20 | 1.5 | 2.0 | 390 | 600 | 120 | 450 | 110 | 800 | .55 |
| 39 | 15 | 2.9 | 3.6 | 240 | 450 | 140 | 240 | 100 | 430 | .45 |
| 41 | 16 | 3.5 | 3.2 | 50 | 300 | 55 | 290 | 80 | 360 | .35 |
| Avg. | 13 | 2.5 | 3.0 | 180 | 390 | 100 | 340 | 120 | 450 | .50 |

The factor 2 in front of $Q_{po}$ in equations (4) and (5) is the so-called "peak factor," accounting for the observation that a visible plume can persist past the point at which the average plume becomes unsaturated. Saturated parcels of air persist in the midst of unsaturated air. The empirical peak factor was first used in the analyses by Meyer et al. (1974), Slawson et al. (1974), and Briggs (1975).

It is seen in Table 2 that the numerical and analytical models are equally capable of estimating the visible plume height and length. The average observed and estimated visible plume length and height agree within 20% and 80%, respectively. More detailed discussions of these comparisons are given in Appendices A and B.

3. St. Louis Refinery Cloud

While measuring cumulus clouds in the vicinity of St. Louis with an instrumented light aircraft, Auer (1976) noticed a cumulus cloud that was obviously forming in the plume from a refinery complex. He made several passes through the cloud, measuring temperature excess, vertical speed, and excess water. He also obtained vertical soundings of dry bulb temperature, dew point, and wind speed. Unfortunately, the source details are sketchy in his report, and it is necessary to arbitrarily choose parameters such as the initial plume radius. Auer states that the refinery gives off $7 \times 10^{11}$ cal $h^{-1}$ (about 800 MW), divided about equally

between sensible and latent heat. For the model calculations the initial plume temperature, relative humidity, radius, and vertical speed are assumed to equal 302.3 K, humidity 76%, 250 m, and 1 m/s, respectively. Initial values of cloud and rainwater content are set equal to zero. The environment profiles are given in Table 3.

Table 3

Profiles of Temperature, Dewpoint, and Windspeed for the St. Louis Refinery Cloud on 10 August 1973 (after Auer, 1976)

| z(m) | Temperature (°K) | Dewpoint (°K) | U(m/s) |
|---|---|---|---|
| 0. | 300.5 | 296.0 | 1.1 |
| 250. | 298.0 | 295.5 | 1.1 |
| 450. | 296.5 | 295.0 | 1.3 |
| 600. | 295.0 | 294.5 | 1.8 |
| 750. | 293.5 | 292.8 | 1.9 |
| 900. | 292.5 | 291.0 | 3.0 |
| 1050. | 291.8 | 285.0 | 2.5 |
| 1200. | 290.6 | 288.5 | 2.0 |
| 1350. | 289.4 | 288.5 | 2.0 |
| 1500. | 288.5 | 286.5 | 1.1 |
| 1650. | 287.5 | 286.5 | 2.0 |
| 1850. | 286.0 | 284.2 | 3.8 |
| 2000. | 285.0 | 282.0 | 3.8 |
| 2100. | 284.8 | 278.0 | 3.8 |
| 2250. | 284.0 | 277.5 | 3.8 |
| 2350. | 283.3 | 277.8 | 3.8 |

The comparison of observations with model output are summarized in Table 4 below (all heights are in meters above the surface):

Table 4

Comparison of Observations and Predictions for St. Louis Refinery

| | Observed | Predicted |
|---|---|---|
| Cloud base | 700m | 650m |
| Cloud top | 2050m | 2350m |

| z(m) | Liquid Water Content Observed ($g/m^3$) | Liquid Water Content Predicted ($g/m^3$) |
|---|---|---|
| 930 | .046 | .56 |
| 1270 | .10 | .75 |
| 1860 | .44 | 1.30 |

| z(m) | Observed w(m/s) | Predicted w(m/s) |
|---|---|---|
| 500 | 3 | 2.0 |
| 1500 | 4 | 2.0 |
| 2000 | 3 | 2.3 |

| z(m) | Observed $(T_p-T_e)$(°K) | Predicted $(T_p-T_e)$°K |
|---|---|---|
| 500 | .2 | .1 |
| 1500 | -.5 | .3 |
| 2000 | -.2 | .5 |

The height of the cloud base and top are quite well predicted by the model. There is a slight inversion above about 2100 m which causes the plume to level off. The predicted vertical speed w is about a factor of two too low at all heights and the predicted liquid water content is a factor of three to ten too high. The observed and predicted temperature



AWS TECHNICAL LIBRARY
FL 4414
859 BUCHANAN STREET
SCOTT AFB IL 62225-5118

differences are within 1°K of each other. Because of the differences in water vapor content between the plume and the environment, the virtual temperature difference ($T_{pv}-T_{ev}$) is positive even though the observed actual temperature difference is negative at heights of 1500 and 2000m.

Auer calculated the entrainment rate based on his measurements of temperature in the cloud. He finds that the entrainment rate is between 33 and 91%/km for eight different passes through the cloud. In the numerical model the entrainment rate $(1/V)(dV/dz)$ equals $0.8/R$, where V is the volume flux, $UR^2$. Thus the theoretical entrainment rate is about 160% at cloud base and about 75% at a height of 2000 m (using $R = R_o + 0.4z$). There is a great deal of uncertainty among the cloud modelers with respect to their recommendations of entrainment rate for cumulus clouds (see Cotton, 1975). It is measurements such as Auer's which will allow modelers to better specify the entrainment rate.

4. Rancho Seco Cooling Towers

The plumes from the two natural draft cooling towers at the Rancho Seco, California, nuclear power plant were sampled by Wolf (1976a) using a light aircraft. Environmental data from the three days of measurements are listed in Table 5.

The two towers have radii of 30 m and their centers are separated by 140 m. In the model, a single plume is followed to a height where its radius equals 70 m, or one half of the distance between the towers. Beyond this point, the plumes are assumed to merge and the fluxes of all parameters increase by a factor of two. The measured initial velocities, $w_o$, on the three days

Table 5

Environmental Data from Rancho Seco, California (from Wolf, 1976b)

| Height above tower (m) | 2/17/75 $T_e$ (1) | 2/17/75 $T_d$ (2) | 2/17/75 U (3) | 2/18/75 $T_e$ | 2/18/75 $T_d$ | 2/18/75 U | 2/20/75 $T_e$ | 2/20/75 $T_d$ | 2/20/75 U |
|---|---|---|---|---|---|---|---|---|---|
| 0 | 280.0 | 270.9 | 5.0 | 283.0 | 274.4 | 3.4 | 283.2 | 275.4 | 9.1 |
| 44 | 279.5 | 270.6 | 5.0 | - | - | - | 282.8 | 274.8 | 9.0 |
| 120 | 278.8 | 270.9 | 5.0 | 281.5 | 273.7 | 2.8 | 282.0 | 274.7 | 8.8 |
| 197 | 278.2 | 270.0 | 5.0 | - | - | - | - | - | - |
| 273 | 278.9 | 268.9 | 5.6 | 280.4 | 272.3 | 2.2 | 280.6 | 273.4 | 8.2 |
| 425 | 279.2 | 265.3 | 7.2 | 279.5 | 269.9 | 1.9 | 279.2 | 271.2 | 7.1 |
| 578 | 278.4 | 266.8 | 9.4 | 278.5 | 267.1 | 1.5 | 277.9 | 271.3 | 6.0 |
| 654 | - | - | - | 277.8 | 267.2 | 1.8 | - | - | - |
| 730 | 278.0 | 264.7 | 11.0 | 278.0 | 268.6 | 2.4 | 276.6 | 270.1 | 5.0 |
| 807 | - | - | - | 278.1 | 267.7 | 2.9 | - | - | - |
| 883 | - | - | - | 278.0 | 266.5 | 3.0 | 276.1 | 269.0 | 4.5 |

(1) Dry bulb temperature, °K.

(2) Dewpoint, °K.

(3) Wind Speed, from pilot balloons (m/s)

2/17, 2/18, and 2/20, are 4.4, 3.6, and 3.9 m/s, respectively. Wolf suggests that the initial liquid water content should be less than we have been using previously, since he has measured liquid water concentrations no greater than .0001 g/g at a distance of 125 m from the tower exits. Therefore, for these three runs, it is assumed that $Q_{co}$ equals .0005 and $Q_{Ho}$=.0001 g/g. Equations (2) and (3), based on the John E. Amos towers, were used to estimate the initial plume temperatures.

The estimated visible plume length and height are compared with observations in Table 6.

Table 6

Observed and Estimated Visible Flume Length and Height at Rancho Seco

| | Feb 17 | | Feb 18 | | Feb 20 | |
|---|---|---|---|---|---|---|
| | obs. | model | obs. | model | obs. | model |
| Plume length (m) | vert. | 170 | 500 | 130 | 1000 | 250 |
| Plume height (m) | 350 | 110 | 800 | 160 | 420 | 75 |

It is seen that the model underestimates visible plume length and height by a factor of three to five. However, Wolf reports that he observed visible plumes when the average plume relative humidity was as low as 60%. Either the plume is far lumpier than we think, or the measured relative humidities are too low. If the former is true, the model could be improved by increasing the peak factor.

The observed and estimated excess temperature and excess water content are in better agreement than the visible plume parameters, as seen in Table 7. The observed temperature excess is about twice the estimated excess, on the average. The observed and estimated excess water content are generally quite close. The paradox exists that visible plume length is not estimated very well, while excess water content is estimated quite well. Adjustments in the peak factor cannot simultaneously improve predictions of visible plume length and excess water content at Rancho Seco.

5. Climatology of Plume Types

Since the plume and cloud growth model is relatively simple and each computer run costs only a few cents, it is feasible to apply the model to large numbers of input data. The statistics of the resulting plume predictions can be calculated and a climatology of plume types developed. The average plume rise and visible plume length and height for a year and for various seasons can be included in the climatology. Plume characteristics for weather categories ranging from clear to precipitation can be estimated.

Upper air and surface observations from the Nashville weather service office for the months January, April, July, and October, 1974, were obtained. Since observations are taken twice each day

Table 7

Observed and Estimated Temperature and Water Content Excesses at Rancho Seco

| Date | Height above tower (m) | $(T_p-T_e)$(°K) obs. | $(T_p-T_e)$(°K) model | $(q_p+Q_c+Q_H-q_e)$(g/kg) obs. | $(q_p+Q_c+Q_H-q_e)$(g/kg) model |
|---|---|---|---|---|---|
| Feb 17 | 120m | 7.2°K | 2.3°K | 5.1 g/kg | 3.3 g/kg |
| | 136 | 5.6 | 2.0 | 3.6 | 3.1 |
| | 151 | 5.0 | 1.6 | 3.1 | 2.8 |
| | 181 | 1.9 | 1.2 | 1.8 | 2.5 |
| | 273 | 2.3 | -.3 | 2.1 | 1.8 |
| | 349 | 0.7 | top at 340m | 1.1 | |
| Feb 18 | 197m | 2.2°K | 1.3°K | 2.2 g/kg | 3.2 g/kg |
| | 273 | 2.1 | 0.7 | 2.4 | 2.4 |
| | 425 | 0.8 | -0.1 | 1.8 | 1.9 |
| | 578 | -0.3 | -0.5 | 0.8 | 1.7 |
| | 730 | -0.5 | top at 610m | 0.4 | |
| | 883 | -2.1 | | 0.4 | |
| | 974 | -3.8 | | 0 | |
| Feb 20 | 120m | 3.0°K | 1.3°K | 1.9g/kg | 2.6g/kg |
| | 151 | 3.0 | 0.9 | 2.0 | 2.0 |
| | 181 | 1.4 | 0.7 | 0.8 | 1.7 |
| | 273 | 0.9 | 0.4 | 0.6 | 1.2 |
| | 425 | 0 | 0.1 | 0.4 | 1.1 |
| | 486 | 1.0 | 0 | 0.7 | 0.9 |
| | 730 | -0.4 | top at 720m | -0.1 | |

(morning and evening), a total of 241 sets of input data are used. The Nashville station was chosen because of its proximity to the proposed TVA Hartsville power park, the surrogate nuclear energy center site at Land-Between-the Lakes, and the existing TVA Paradise steam plant.

The four different types of sources used as input to the model are listed in Table 8.

Table 8

Source Input for Plume Climatology Study

| Approximate power | Number of cooling towers | $w_o$(m/s) | $T_o$(°K) | $R_o$(m) | Characteristics |
|---|---|---|---|---|---|
| 1000 MW | 1 | 4.4 | (eq 2) | 30 | Typical natural draft tower. |
| 10000 MW | 1 | 4.4 | (eq 2) | 92 | Same, but larger diameter. |
| 100000 MW | 1 | 4.4 | (eq 2) | 300 | Same, but much larger diameter. |
| 100000 MW | 100 | 4.4 | (eq 2) | 30 | Square grid. Groups of four towers, with the towers spaced 200m apart Groups are spaced 1 km apart. |

Because the model is one dimensional, plume merging in the 100000 MW power park with 100 cooling towers must be completely parameterized. It is assumed that the four plumes in a group merge if the plume radius equals 100m (one half of the distance between the towers) and the groups merge if the plume radius equals 500m (one half of the distance between the groups). The other source types in the

table are treated as if all the heat were from one cooling tower. This is unrealistic for the 10000 and 100000 MW sources, but will provide estimates of the worst possible cases of weather modification.

5.1 Plume Rise

Final plume rise is defined as the height at which the vertical speed of the plume, w, reaches zero. In about one-third of the runs for the single 1000 MW tower, a cloud exists ($Q_C+Q_H>0$) at the height of final plume rise. This fraction increases to 95% for the single $10^5$ MW tower. The average plume rise for the four different months and four different sources are listed in Table 9. The numbers in parentheses are the range of plume rise for that class.

The increase in plume rise with increase in source strength for the first three types of sources is in approximate agreement with Briggs' (1975) theory for plume rise, which predicts that the plume rise for bent over plumes is proportional to source strength raised to the one third power. The figures for average annual plume rise show that the ratio of the $10^4$ MW plume rise to the $10^3$ MW plume rise is 2.04 and the ratio of the $10^5$ MW plume rise to the $10^3$ MW plume rise is 4.25. Briggs' theory predicts that these ratios will be $10^{1/3}$, or 2.15, and $100^{1/3}$, or 4.65, respectively.

Table 9

Average Plume Rise Estimated Using Nashville Radiosonde Observations.
The Range in Plume Rise for that Class is Given in Parentheses.

| Month (all 1974) | Morning Rise (m) | | | | Evening Rise (m) | | | | Average Rise (m) | | | |
|---|---|---|---|---|---|---|---|---|---|---|---|---|
| | $10^3$MW | $10^4$MW | $10^5$MW | $10^5$MW spaced | $10^3$MW | $10^4$MW | $10^5$MW | $10^5$MW spaced | $10^3$MW | $10^4$MW | $10^5$MW | $10^5$MW spaced |
| Jan. | 500 (160-1340) | 880 (320-1450) | 1470 (650-3600) | 610 (160-1390) | 660 (240-1360) | 970 (400-1690) | 1590 (750-4010) | 740 (240-1530) | 580 (160-1360) | 920 (320-1690) | 1530 (650-4010) | 670 (160-1530) |
| Apr. | 490 (170-1430) | 1030 (300-1920) | 2340 (780-4500) | 610 (170-1740) | 890 (120-1600) | 1410 (190-2160) | 2550 (420-4300) | 1090 (120-1880) | 690 (120-1600) | 1220 (190-2160) | 2440 (420-4500) | 850 (120-1880) |
| July | 470 (200-1590) | 1530 (340-3110) | 3130 (1260-4950) | 890 (210-3620) | 730 (240-1800) | 1590 (520-2710) | 3570 (1690-5460) | 1130 (240-2980) | 600 (200-1800) | 1500 (340-3110) | 3250 (1260-5460) | 1010 (210-3620) |
| Oct. | 360 (190-990) | 850 (320-3160) | 2410 (850-4790) | 420 (230-1200) | 550 (260-1140) | 1140 (500-2160) | 2610 (1500-4600) | 770 (210-2300) | 450 (190-1140) | 1000 (320-3160) | 2510 (850-4790) | 600 (210-2300) |
| Avg. annual | 450 (160-1590) | 1030 (300-3160) | 2340 (650-4950) | 630 (160-3620) | 710 (120-1800) | 1280 (190-2710) | 2580 (420-5460) | 930 (120-2980) | 580 (120-1800) | 1180 (190-3160) | 2460 (420-5460) | 780 (120-3620) |

The spaced $10^5$ MW energy center yields an average plume rise between those for the single $10^3$ MW tower and the single $10^4$ MW tower. Occasionally, the plumes will combine and yield a plume rise close to that for the single $10^5$ MW tower. In about 90% of the runs, the four towers in a group merge, and in about 15% of the runs, the 25 groups merge. But since merger generally occurs near the top of the plume, it doesn't give the plume much additional boost. A general rule for avoiding plume merger is to space the cooling towers a distance apart equal to the average plume rise from a single tower. In this way, the plume radii, which grow roughly as .4z, do not reach the critical value for plume merger (one-half the distance between the towers).

The enhancement of plume rise due to the merging of multiple plumes has been predicted theoretically by Briggs (1974). The ratio of the enhanced plume rise from N sources to the plume rise from one source, which is denoted by $E_N$, is a function of the number of sources, N, the plume rise from one source, H, and the distance between the sources, s.

$$E_N = ((N + S)/(1 + S))^{1/3} \qquad (7)$$

where $S = ((N-1)s/N^{1/3}H)^{3/2}$

From the results in Table 9, it can be assumed that H is 580 m. For the small groups in our hypothetical power park (N = 4 and s = 200m), $E_N$ equals 1.43. For the entire power park (N = 100 and s = 1000m), $E_N$ equals 1.14. In this case the enhancement factors for the groups of four and the entire power park should probably be multiplied together. Thus the theoretical enhancement $E_N$ is predicted to be about 1.4 or 1.5 for our hypothetical power park. The plume and cloud growth model yields the result that the average annual ratio of plume rise for the $10^5$ MW spaced power park to the plume rise for the single $10^3$ MW cooling tower is 780m/580m, or 1.35.

The seasonal variation of plume rise in Table 9 is what would be expected intuitively, with the lowest plume rise usually occurring during the winter when the lower atmosphere is more stable. Similarly, the afternoon plume rises are 10 to 80% greater than the morning plume rises. The diurnal variation is less for the large sources, since the morning inversion is usually limited to a layer about 100 to 200 m deep near the ground. However, the annual variation is greatest for the large sources, presumably due to the influence of the deep isothermal or inversion layers which exist during the winter. Also, it should be stressed that this "climatology" is based on observations during only four months. Ideally, observations during at least ten years should be used to establish a stable climatology.

## 5.2 Cloud at Top of Plume

In many model calculations, liquid water exists in the plume at the height of final rise. Either a cloud persists from the tower opening through the entire depth of the plume, or it forms just above the lifting condensation level, with clear air beneath it. The frequencies of cloud occurrence for the six weather classes are given in Table 10, where the source is the single 1000 MW, 30 m radius tower. On the average, a cloud is predicted at the top of the plume 39% of the time. During precipitation, fog, or cases when the cloud height is less than 10,000 ft., a cloud is predicted about 60% of the time. Clouds are very unlikely during afternoons which are clear or have high clouds. The reason that such high occurrence of clouds are not reported from operating cooling towers is that on foggy days or days with precipitation it is hard to see the plume. The model calculates plumes on all days, instead of just sunny days when the observer can easily see the plume.

Table 10

Frequency of Cloud Occurrence (QCO + QHO>0 at Height of Final Rise) for 1000 MW Tower at Nashville

| Weather Class | Observed class freq. am | pm | Frequency of cloud occurrence within class am | pm |
|---|---|---|---|---|
| 1. Clear | .09 | .15 | .32 | 0 |
| 2. Precipitation | .18 | | .60 | |
| 3. Cloud height ≥ 20,000 ft. (no prec.) | .05 | .07 | .23 | 0 |
| 4. 10,000 ≤ cloud height < 20,000 ft. (no prec.) | .09 | | .14 | |
| 5. Cloud height < 10,000 ft. (no prec.) | .24 | | .53 | |
| 6. Fog (no prec.) | .13 | | .65 | |
| All | 1.00 | | .39 | |

The frequency of cloud occurrence is predicted to increase as source size increases, as shown in Table 11.

Table 11

Frequency of Cloud Occurrence Estimated
Using Nashville Radiosonde Observations

| Month (all 1974) | $10^3$MW | $10^4$MW | $10^5$MW | $10^5$MW spaced |
|---|---|---|---|---|
| Jan. | .41 | .70 | .97 | .59 |
| Apr. | .34 | .59 | .96 | .43 |
| July | .51 | .76 | .97 | .59 |
| Oct. | .31 | .54 | .89 | .39 |
| Total | .39 | .64 | .95 | .50 |

For the $10^5$ MW spaced power park the frequency of cloud occurrence is roughly halfway between those for single $10^3$ MW and $10^4$ MW cooling towers. As seen in Table 9, the plume rise for the spaced power park occupies the same relative position between that for the single $10^3$ MW and $10^4$ MW towers. A cloud forms nearly all the time (frequency .95) over the single $10^5$ MW cooling tower. This is a good argument against clustering the waste heat sources as close together as possible. This model predicts that a cloud averaging 2500 m deep would exist nearly continuously over an area with radius 300 m dissipating $10^5$ MW of heat.

## 5.3 Liquid Water Content of Cloud Formed by Cooling Tower

The liquid water content of a cloud determines the visibility in the cloud and the rainfall rate from the cloud. The removal of large raindrops from the plume is calculated using a scheme developed by Simpson and Wiggert (1969), but it is uncertain whether the estimated rainfall rate at the ground is realistic. A cooling tower cloud is unlike a natural cloud in that its base is stationary rather than drifting with the wind.

The average liquid water contents listed in Table 12 refer to only those cases when a cloud formed at the top of the plume. The average liquid water contents range between .29 and .63, in agreement with typical values reported by Fletcher (1962) of the liquid water content in natural clouds. The peak liquid water content is 1.49 g/kg. It is seen that the average liquid water content for the larger sources is significantly greater than that for the $10^3$ MW source, but that there is no significant seasonal variation. In most cases the liquid water content at the top of the plume is less than that in the middle sections of the cloud.

Table 12

Average and Peak Concentration of Cloud Water at the Top of Plumes Which are Condensed at the Height of Final Rise, Estimated Using Nashville Radiosonde Observations.

| Month (all 1974) | Average Concentration (g/kg) $10^3$MW | $10^4$MW | $10^5$MW | $10^5$MW spaced | Peak Concentration (g/kg) $10^3$MW | $10^4$MW | $10^5$MW | $10^5$MW spaced |
|---|---|---|---|---|---|---|---|---|
| Jan. | .40 | .54 | .62 | .47 | .72 | .96 | 1.49 | .98 |
| Apr. | .44 | .60 | .61 | .54 | .82 | 1.15 | 1.19 | 1.00 |
| July | .29 | .63 | .44 | .49 | .91 | 1.03 | .77 | 1.25 |
| Oct. | .33 | .39 | .44 | .36 | .62 | 1.02 | 1.09 | .90 |
| Total | .36 | .54 | .53 | .47 | .91 | 1.15 | 1.49 | 1.25 |

## 5.4 Relation of Plume Rise to Inversion Height

Based on observations of cooling tower plume rise on cold winter mornings at the John E. Amos power plant Brennan et al. (1975) state that the capping inversion height, or mixing layer depth, determines the final plume rise. In Section 2 and in Hanna (1976a), it is pointed out that this conclusion is not likely to be valid during the summer, when the capping inversion is much higher than it is in the winter. Consequently the 241 Nashville runs were analyzed to determine the relation between plume rise from the 1000 MW cooling tower and inversion height.

A well-defined capping inversion is found in 89 of the runs, with the average plume rise and inversion height during these conditions equal to 690 m and 1250 m, respectively. All the runs are summarized in Table 13. The correlation coefficients between plume rise and inversion height are seen to be very high for the group of runs where the estimated plume rise is greater than or equal to the inversion height. If the plume has enough buoyancy to bring it to the capping inversion, it will in all likelihood stop there.

Table 13

Plume Rise and Capping Inversion Height for the 1974 Nashville Soundings. The Number of Runs in Each Category is Given in Parenthesis.

| Month | Avg. Capping inversion height | Avg. Model plume rise | Correlation Coefficient between Capping Inversion Height and Plume Rise | |
|---|---|---|---|---|
| | | | All runs with inversion | Runs with plume rise≥inversion height |
| Jan. | 920m | 640m | .31(39) | .989(14) |
| Apr. | 1640 | 760 | .20(25) | .998(5) |
| July | 1700 | 1250 | .78(5) | (0) |
| Oct. | 1280 | 570 | .15(20) | (2) |
| Total | 1250 | 690 | .33(89) | .993(21) |

## 5.5 Visible Plume Length

The model calculations stop after the vertical speed of the plume falls to zero. Downwind of this point, where passive diffusion governs the distribution of excess water, very little is known about cooling tower plumes. It is better to wait for the results of measurement programs than to go ahead with a completely arbitrary model of passive diffusion. Consequently, this section on visible plumes is concerned only with plumes which evaporate before they reach the height of final rise. With this restriction, for the single 1000 MW source, the average annual visible plume height is 150 m and the average annual visible plume length is 190 m. These estimates are about a factor of two less than the observations of visible plume geometry at the Paradise cooling towers, where the average annual visible plume height is 280 m and the average annual visible plume length is 390 m. At Paradise there are three cooling towers with a total energy output of more than 2000 MW. Our analysis of the daily Paradise observations is continuing in order to compare the model predictions of plume rise and visible plume length with the observations for the classes of weather conditions listed in Table 10.

Seasonal variations of predicted visible plume length and height are given in Table 14. It is seen that the average resultant visible plume length is about 40% to 75% longer in January than in July, and that the morning length is about twice as long as the afternoon length. Furthermore, the angle of the plume with the horizontal is about 30° less in the winter than in the summer,

presumably due to the greater wind speeds in the winter (8.0 m/s in January compared to 3.4 m/s in July). The shortest plumes occur on hot dry days in July, when the visible plume length is only about 50 m, or about one tower diameter.

Table 14

Visible Plume Length and Height Predicted Using Nashville Radiosonde Observations, for Plumes which are not Visible at their Final Height of Rise. The Resultant Plume Length is the Hypotenuse formed by the Visible Plume Length and Height.

| Month | Height(m) | | Length(m) | | Resultant(m) | |
|---|---|---|---|---|---|---|
| | am | pm | am | pm | am | pm |
| Jan. | 230 | 130 | 430 | 170 | 490 | 210 |
| Apr. | 180 | 90 | 330 | 130 | 380 | 160 |
| July | 240 | 120 | 140 | 90 | 280 | 150 |
| Oct. | 240 | 80 | 210 | 110 | 310 | 140 |
| Average | 220 | 100 | 280 | 130 | 360 | 160 |

## CHAPTER III

# PLANS FOR LABORATORY STUDY OF FLOW AND PLUME BEHAVIOR NEAR SINGLE AND MULTIPLE COOLING TOWERS OF VARIOUS TYPES

by
R.P. Hosker, Jr.

## 1. Introduction

In order to realistically mathematically model and predict the behavior and environmental interactions of cooling towers and their plumes, a certain amount of physical insight into the details of the associated phenomena is essential. Laboratory and field studies, as well as providing this requisite understanding of the physics, can also provide the data needed for validation of the resulting mathematical models. From an engineering point of view, such empirical studies can also furnish a great deal of information on phenomena which can significantly affect cooling tower performance (and hence overall power plant efficiency), such as plume downwash, reingestion, and mutual interference effects within tower clusters.

The reporting of such experimentally-derived information is relatively recent in the open literature. Aynsley and Carson (1973) remark, for example, that only twelve papers devoted to cooling tower plumes had been published prior to 1969. Since then, however, research interest in cooling towers has grown enormously. Most of the references to major field and laboratory programs both within the U.S. and abroad can be found in the proceedings of a 1974 symposium (Cooling Tower Environment-1974), and in an excellent critical

review by McVehil and Heikes (1975). The paper of Meyer et al. (1974) is particularly noteworthy because of its very detailed field observations of plume behavior. More recent field studies have been reported by Kramer et al. (1975), Brennan et al. (1976), Norman et al. (1976), and Wolf (1976a).

Few reports on laboratory modeling of cooling towers and their plumes have appeared in the open literature until recently. The contributions of Kennedy and his colleagues (Kennedy and Fordyce, 1974; Bugler and Tatinclaux, 1974) and of Onishi and Trent (1976) are of considerable interest. A study by Symes and Meroney (1970), though not originally intended for cooling tower use, has important implications for near-tower plume behavior.

A review of the above publications indicates several research topics important for the development of realistic mathematical models for cooling tower and plume behavior. In particular, McVehil and Heikes (1975) suggest that, as a practical matter, the most significant cooling tower effects may very often be highly localized problems associated with aerodynamic interactions between the tower, its surroundings, the plume, and the atmosphere. Similarly, in a discussion of Meyer et al. (1974)'s data, Briggs (1974) remarked that "building effects" seemed to be the strongest influences on plume behavior other than those taken into account by relatively simple plume rise models. And Carson (1974), in a discussion of research

required for evaluation of both mechanical and natural draft cooling tower effects, commented on the need for plume models which can include the effects of relative tower orientation, aerodynamic downwash, and other such interactions. Criteria for the atmospheric conditions under which downwash and recirculation may be expected are also necessary, especially for cases involving arrays of towers; such information may provide guidance for avoiding or minimizing these problems by proper design and operation practices.

Experimental work on these unresolved near-tower problems is probably most easily accomplished by laboratory modeling, and this is the primary approach to be taken at ATDL. In the following sections, the requirements for reasonably accurate laboratory simulation of cooling tower and plume behavior will be briefly examined and used to establish the general size and operating conditions of the necessary flow facility. A detailed description of equipment already purchased or about to be procured is given. A list and a tentative timetable are presented for the sequence of cooling tower experiments planned for this facility in Chapter IV.

## 2. Similarity Criteria

### 2.1 General Background

A number of authors (Cermak et al., 1966; McVehil et al., 1967; Ludwig et al., 1971; Snyder, 1972; Lin et al., 1974; Kennedy and Fordyce, 1974; among others) have considered the conditions under

which a fluid (either gas or liquid) model of a given flow situation can provide physically realistic results. These similarity conditions are conveniently obtained by a dimensional analysis of the governing equations (Navier-Stokes, or an approximation of them) together with the proper initial and boundary conditions on the flow.

The procedure, which will only be summarized here, first requires writing out the conservation equations applicable to the atmospheric boundary layer. Mass, momentum, and energy are to be conserved. Viscous, rotational, and gravitational effects must be taken into account. Equations describing the dispersion of (possibly reactive) contaminants within the main fluid must also be given. In addition, the initial and boundary conditions of the real flow must also be explicitly formulated.

The resulting set of coupled, nonlinear, partial differential equations together with the boundary and initial conditions must then be nondimensionalized. This is often done by choosing characteristic values for the dependent variables, such as velocity, temperature, and effluent concentration, so that their nondimensional values are unity or less over the entire flow field. Convenient characteristic values of length and time can be chosen so that either the nondimensional independent variables(time and the spatial coordinates) are of order unity or less, or the nondimensional gradients of these variables are of order unity or less. If the

scales of certain phenomena are very dissimilar--eg, mean velocity and turbulent fluctuations--then two characteristic values may be appropriate. For example, the mean velocity may be scaled by the geostrophic wind speed, while the turbulent velocity components may be normalized with a typical root-mean-square value for one of the components.

In the new set of nondimensional equations and boundary conditions, certain terms are preceded by nondimensional coefficients. A model of the atmospheric boundary layer must, to be physically realistic, obey the same equations as does the natural flow. In particular, the nondimensional coefficients appearing in the governing equations and boundary conditions should be equal in both the model and the atmosphere. In practice it is impossible to obtain such equality of parameters, and so the model is not an exact simulation of the real flow. The question of just how closely the various parameters must be duplicated to produce a reasonable amount of accuracy in a practical model has been the subject of considerable work and discussion (see the authors listed above). Many of their conclusions are utilized in the discussion below.

The nondimensional parameters which arise from the conservation equations for mass, momentum, and energy are the Reynolds number, the bulk Richardson number (the inverse square of the overall densimetric Froude number), the Rossby number, the Prandtl number, and the Eckert number. The equation describing diffusion of a

passive effluent within the main fluid gives rise to the Schmidt number.

The Prandtl and Schmidt numbers occur in the equations as products with the Reynolds number. These products can be physically interpreted as the ratio of the heat or effluent, respectively, transferred per unit area in unit time by advection to that quantity transferred by molecular diffusion. The Eckert number appears in the energy equation divided by the Reynolds number; this expression indicates the ratio of the heat generated over a unit area in unit time by viscous forces to that transferred by advection. In the atmospheric boundary layer, molecular-scale diffusion processes are nearly always negligible compared to turbulent diffusion. As long as the model flow is also highly turbulent, similarity of the Prandtl, Schmidt, and Eckert numbers should not be necessary for good model accuracy.

The Rossby number is a measure of the relative importance of inertial and Coriolis forces. The Coriolis force is responsible for the gradual turning of the wind vector with height (the so-called "Ekman spiral"). Near the surface, however, this turning is not significant. An estimate of the thickness of the surface layer within which the Coriolis effect is negligible to within, say, 10% can be made using Lettau's (1962) model for the wind spiral.

This height is about 50m except in low winds, at high latitudes, or over rough terrain; for moderate to strong winds over most surfaces the layer of negligible Coriolis effect should be 100m or more in thickness. For diffusion modeling within the surface layer one should therefore be able to neglect the Rossby similarity requirement. For elevated sources or for diffusion over great distances, however, the effect may become important. Snyder (1972) has surveyed the diffusion literature and concluded that the Coriolis force significantly affects dispersion results when the horizontal distance of travel is more than 5 km for elevated releases, and more than 12 km for ground-level sources.

The bulk Richardson number expresses the ratio of buoyant to inertial forces for the overall flow field, and is especially significant, therefore, at low wind speeds. Since it is a measure of atmospheric stability and hence of the degree of mixing possible, it can be expected to be an important parameter in model studies involving diffusion.

The Reynolds number represents the relative importance of inertial and viscous forces in the flow. A large Reynolds number suggests that viscous effects should be negligible; this is largely true within the bulk of the fluid. However, in regions (e.g., near obstacles) where large velocity gradients are present, viscous shear profoundly affects the overall flow patterns through its influence on boundary layer development, transition and separation, and wake behavior. Since these phenomena can introduce very large perturbations of the flow field which would exist in

the absence of viscosity, the Reynolds number is an important parameter in any modeling effort.

The nondimensional conditions imposed at the various fluid boundaries impose further constraints on the model flow (see, for example, Ludwig et al., 1971; Snyder, 1972; Kennedy and Fordyce, 1974). Geometric similarity is perhaps the most obvious requirement; all stack and building dimensions and distances must be correctly scaled. The nondimensional wind speed and temperature spatial distributions must be duplicated at the upwind boundary of the region of modeling interest; both the mean and the fluctuating portions of these quantities should be reproduced in the model. The buoyancy of effluents emitted into the modeled region must be taken into account by matching the effluent densimetric Froude numbers to those of the prototype. Similarly, initial momentum effects in plumes can be properly simulated only if the prototype ratios of efflux velocity to ambient wind speed are reproduced in the model.

## 2.2 Application to Cooling Tower Modeling

If the situations to be modeled concern only the near-field behavior of cooling towers and their plumes, then a number of the above-mentioned similarity requirements are unimportant and may be neglected in the modeling effort. Others may be relaxed.

For example, since the horizontal region of interest will extend less than a kilometer or so, the earth's rotation will have no significant effect on the plume, and the Rossby number criterion may be omitted.

A chief concern of this modeling study will be the interaction between plumes and cooling towers. Phenomena such as strongly bent over plumes, downwash, recirculation, and mutual interference between tower arrays are produced mainly by the aerodynamic flow fields around the towers themselves. Such effects are especially important during periods of strong winds, which commonly occur during conditions of neutral or near-neutral atmospheric stability. The present investigation will therefore be confined to such circumstances, during which the bulk Richardson number is nearly zero. A model flow with no corrections for ambient atmospheric stability should hence be adequate.

The Reynolds number in the atmosphere is typically very large--$10^5$/m to $10^6$/m of characteristic length L. Its definition, $Re \equiv UL/\nu$, suggests that a reduction in L might be properly compensated by an increase in characteristic wind speed U and/or a decrease in the fluid kinematic viscosity $\nu$. However, sizeable scale reductions, on the order of 1/100 or more are necessary to reduce large structures such as cooling towers to reasonable laboratory dimensions. Furthermore, buoyant plume modeling requirements restrict U to as small a value as practicable, as discussed below. Hence it will in general not be possible to match Reynolds numbers in the model and prototype flows. This difficulty is sidestepped by an appeal to the concept of "Reynolds number independence" introduced by Townsend (1956). McVehil et al. (1967) and Snyder (1972) have reviewed some of the pertinent ideas; the situation may be summarized as follows.

In the nondimensional momentum equations of fluid flow, the terms describing viscous effects are preceded by the coefficient 1/Re, indicating that in the atmosphere, where Re is large, the flow must be nearly viscosity independent away from zones of strong velocity gradients. Furthermore, atmospheric flows are nearly always "fully aerodynamically rough" (Sutton, 1953); that is, the surface irregularities and the flow speeds are both sufficiently large that no laminar boundary sublayer exists at the surface (Sutton, 1953; Schlichting, 1960). Consequently even the flow close to the surface is nearly viscosity-independent. As regards the turbulent structure of the flow, all of the large energy-containing eddies and probably most of the intermediate-sized eddies are also independent of viscosity (Townsend, 1956). The smallest eddies present in the flow, however, dissipate kinetic energy by viscous action and must necessarily be Reynolds number dependent (Landau and Lifshitz, 1959). In other words, at large Reynolds numbers both the mean flow and most of the turbulent structure will be invariant with changes in Re; only the small-scale structure in which energy dissipation occurs varies with Re. The latter feature is relatively unimportant for structural and diffusion modeling.

The key to successful modeling of neutrally stable atmospheric flow phenomena (excluding those in the energy dissipation scale) is thus to insure that the model flow is likewise independent of Reynolds number--ie, that a "critical" Reynolds number is exceeded

in the model. This critical value, at which the flow becomes fully rough over the various surfaces, can be determined from the criterion (Sutton, 1953) $u_* z_o/\nu \geq 2.5$, where $z_o$ is the surface's aerodynamic roughness length and $u_* \equiv \sqrt{\tau_w/\rho}$ is the friction velocity determined from the wall shear stress $\tau_w$. The critical value may also be empirically determined by observing larger scale flow phenomena such as boundary layer separation and reattachment points, and wake behavior; these will cease to change when the critical Reynolds number is reached. For sharp-edged structures these features may be largely fixed by the geometry, leading to relatively small values for Re critical; for example, Golden's (1961) experiments suggest Re critical $\simeq$ 11,000 for a cube. Rounded structures, on the other hand, must rely on the flow itself to establish separation points, and the critical values will hence be larger. Halitsky et al. (1963) found Re critical > 79,000 for a typical smooth reactor shell model. Increased roughness of the model surfaces, as well as devices such as boundary layer trips could lower these values (Schlichting, 1960; Halitsky, 1968). Premature separation can also be artificially controlled by means such as boundary layer suction or blowing (Goldstein, 1965).

As an example, consider a hypothetical mechanical draft cooling tower consisting of a box-like structure 20mx20mx12m high, surmounted by a pair of roughly cylindrical stacks 10m in diameter x7m high. The characteristic length L for the box is taken as the square root of its projected area, while that for a stack is taken as its diameter. For a model scale of 1/150, in air, a characteristic

speed U ≃ 1.6 m/sec yields Re ≃ 11,000, which would satisfy Golden's (1961) lower bound for cubical structures. However, Re for one of the stacks under these conditions is only a bit over 7,000--probably far too small for naturally induced separation to occur at a location similar to that in the prototype. Roughening of the stack surface and other such "tricks" would probably be needed to produce a realistic separation point on this model.

The parameters associated with the boundary conditions must now be considered. For the neutrally stable atmospheric flows of interest, the mean velocity profile approaching the modeled zone should be nearly logarithmic in height if the upwind terrain is approximately homogeneous (Pasquill, 1971, for example). In practice this logarithmic profile is often approximated by a power law whose exponent depends on the upwind surface roughness (Davenport, 1963).

It is also necessary to model the turbulence structure of the approaching flow. Since the components of this profile are randomly fluctuating quantities, one can only hope to duplicate the statistics of the turbulence. Townsend (1956) notes that a statistical description of such a turbulent field requires a knowledge of the joint probability distribution function for the components at all spatial points. Once this has been specified, an infinite set of joint moments (i.e., the mean values of products of powers of the various fluctuating components) can be calculated. Conversely, supplying a complete set of measured moments is

equivalent to specifying the distribution function (Lumley and Panofsky, 1964). Hence an accurate model of a turbulent profile should reproduce all the joint moments of the prototype profile. These include, for example, the double, triple, and higher order Eulerian velocity correlation coefficients.

In view of the difficulty, cited by Brodkey (1967), of measuring even triple correlation coefficients, modelers are usually content to match the turbulence intensity profiles for each of the velocity components and the profiles of the various double correlation coefficients, or equivalently, the various spectra. Such matching should not be considered to be a full duplication of the atmosphere's turbulence structure; only the intensity and, in some sense, the size of the turbulent eddies have been reproduced. A number of such attempts have been reported (Davenport and Isyumov, 1967; Sundaram et al. 1972; Peterka and Cermak, 1974; and others). Typical atmospheric data have been reported by, for example, Busch and Panofsky (1968), Gault, Jones, Monson, and their colleagues (1967, 1969, 1970), Izumi (1971), and Izumi and Caughey (1976).

An important similarity parameter for cooling tower modeling is the densimetric Froude number of the effluent, defined as $Fr = W_p/(gd|\Delta\rho/\rho_a|)^{1/2}$, where $W_p$ is the plume efflux velocity,

d is the exit diameter, and $\Delta\rho = \rho_a - \rho_p$ is the difference in density between the atmosphere and the emerging plume. If Fr is small, buoyancy effects will be significant in the modeling. For a mechanical draft cooling tower, Kennedy and Fordyce (1974) found that $2 \leq Fr \leq 7$ for most prototype situations. The data of Slawson et al. (1974) for the natural draft towers at Paradise, KY., give $0.28 \leq Fr \leq 0.60$. Evidently buoyancy effects are more important for natural draft towers, as could be intuitively expected.

Another important cooling tower parameter is the ratio of plume efflux velocity to the ambient windspeed at the exit, $W_p/U_a$. For mechanical draft towers Kennedy and Fordyce (1974) use $0.4 \leq W_p/U_a \leq 12$, while Slawson et al. (1974) give $0.22 \leq W_p/U_a \leq 0.76$ for natural draft towers. Larger values are likely for both types in near-calm atmospheric conditions.

As Hoult et al. (1975) pointed out, the need to duplicate both of these parameters in a cooling tower model bounds the scale reduction which can be used at a specified flow speed or, alternately, limits the flow speed if the model size is prescribed. This can be seen as follows. Combine the expression requiring Fr and $W_p/U_a$ to be equal in both model and field to obtain

$$U_m = Fr(W_p/U_a)_f^{-1}(gd_m|\Delta\rho/\rho_a|_m)^{1/2} \quad , \qquad (1)$$

where the subscripts denote model or field values. The density difference term can be much larger in the laboratory than in the

field if, say, a helium-air mixture is used for the model plume. However, it appears that $|\Delta\rho/\rho_a|_m \leq 0.4$ should be maintained to avoid altering the plume entrainment mechanisms (Hoult and Weil, 1972; Hoult et al., 1975). That is,

$$U_m \leq 1.98 Fr (W_p/U_a)^{-1} (d_f)^{1/2} (d_m/d_f)^{1/2} \quad , \qquad (2)$$

where the ratio $d_m/d_f$ is the scale reduction. The flow speed is also bounded from below by the Reynolds number requirement discussed earlier. Hence for a given model scale reduction, there is only a limited range of tower operating conditions, described by $Fr(W_p/U_a)^{-1}$, that can be successfully modeled. For example, consider a mechanical draft tower whose exit diameter is approximately 8m. Suppose that, for a scale of 1/100, the lowest flow speed for which the external flow is independent of Reynolds number is 1 m/sec. Subject to the restriction (2), this model could be used to simulate tower behavior only for $Fr(W_p/U_a)^{-1} \geq 1.8$.

One last requirement should be placed on the model flow. The effluent plume should be fully turbulent, just as in the prototype. This may occur naturally for sufficiently large exit velocities, or can be induced by roughness elements inside the stack.

## 3. The Modeling Facility

### 3.1 General Considerations

The test facility design was determined partly by the modeling restrictions pointed out above, and partly by the desire to obtain

a moderately versatile easily-used device. Air was selected as the modeling fluid because of our previous experience and the extensive literature available on testing structures in simulated atmospheric flows.

Size evolved from a compromise between the large test section area needed for high Reynolds numbers at low flow speeds, and cost limitations on the wind tunnel and the building required to house it. As discussed above, Re≃20,000 or more should provide a fairly accurate simulation of the flow about a sharp-edged obstruction such as a mechanical draft cooling tower. To permit testing over a wide range of values of $Fr(W_p/U_a)^{-1}$, a low flow speed is needed. If $U_m \simeq 1$m/sec, then the characteristic dimension of the model tower must be 30 cm or more, so that the model's projected area is roughly 0.1 $m^2$. Blockage effects due to the presence of the tunnel walls will be small if the test section area is at least ten times larger (Pope and Harper, 1966); that is, a test section area of 1 $m^2$ would be suitable for this example. This is about the largest test section available in prefabricated wind tunnel units at moderate prices; larger tunnels require special shipping arrangements or on-site construction.

Special techniques are needed to produce the simulated velocity profiles and turbulence characteristics in a wind tunnel of modest length. Many such methods have been tried within the last ten years. A review of the pertinent literature (Lloyd, 1967;

Templin, 1969; Campbell and Standen, 1969; Counihan, 1969; Counihan, 1970; Ludwig et al., 1971; Peterka and Cermak, 1974; and others) suggested that at least 3m of the test section should be reserved for flow "processing". Since only near-field measurements out to a distance of 6 or 8 model heights are planned, a total test section length of about 6m was considered adequate.

Speed requirements were rather simple: a range from less than 1 m/sec to 20 m/sec or more. The mean speed profile in the as-delivered (unmodified) test section was required to be highly uniform everywhere in the test section. Similarly, the turbulence levels in this "clean" test section were required to be very low. The flow speed was required to be easily set, repeatable, and stable to within 1% over periods of ten minutes or more.

Large, door-mounted windows were specified on each side for easy access to the model and for photography. Flow visualization studies are anticipated to be an important part of this research. Fixed windows were therefore specified for the test section ceiling to facilitate overhead photography. Removable floor panels were required to allow rapid changes of flow processing devices such as roughness elements, and to permit easy model changes. A turntable will be installed in one such panel to allow testing at various angles of wind incidence.

3.2 Wind Tunnel Specifications

The above requirements are met by a Wirecomb, Inc. model 1391 wind tunnel equipped with an extra test section module. The major

specifications of this tunnel are listed in table 15, and a sketch of the tunnel is provided in Figure 1.

The wind tunnel arrived in Oak Ridge on May 21, 1976, and is presently stored in the Oak Ridge Associated Universities warehouse until the ERDA-funded building to house it has been constructed at ATDL.

TABLE 15

Wind Tunnel Specifications

| | |
|---|---|
| Type: | Open-circuit, low speed, enclosed test section. |
| Test section size: | Two modules, useable separately or in tandem, each 1mx1mx3m long. Total test section length = 6m. |
| Flow speed: | 1 m/sec or less to 22 m/sec or more. Speed "infinitely" resolvable. |
| Turbulence level: | Longitudinal turbulence intensity <1% with one inlet screen, and <0.5% with three inlet screens. |
| Velocity profile: | Flat within ±1% everywhere in test section except in thin wall boundary layers. |
| Flow stability: | Flow speed constant within ±1% over periods of ten minutes or more. |
| Power and drive: | 30 HP SCR-controlled DC motor driving a 7-blade adjustable pitch fan by V-belts and pulleys. |
| General construction: | Plywood on steel frame modules. Each module caster-mounted. Plexiglas viewing windows. |
| Overall size: | Inlet approximately 2.6m square; overall length approximately 13.2m. |

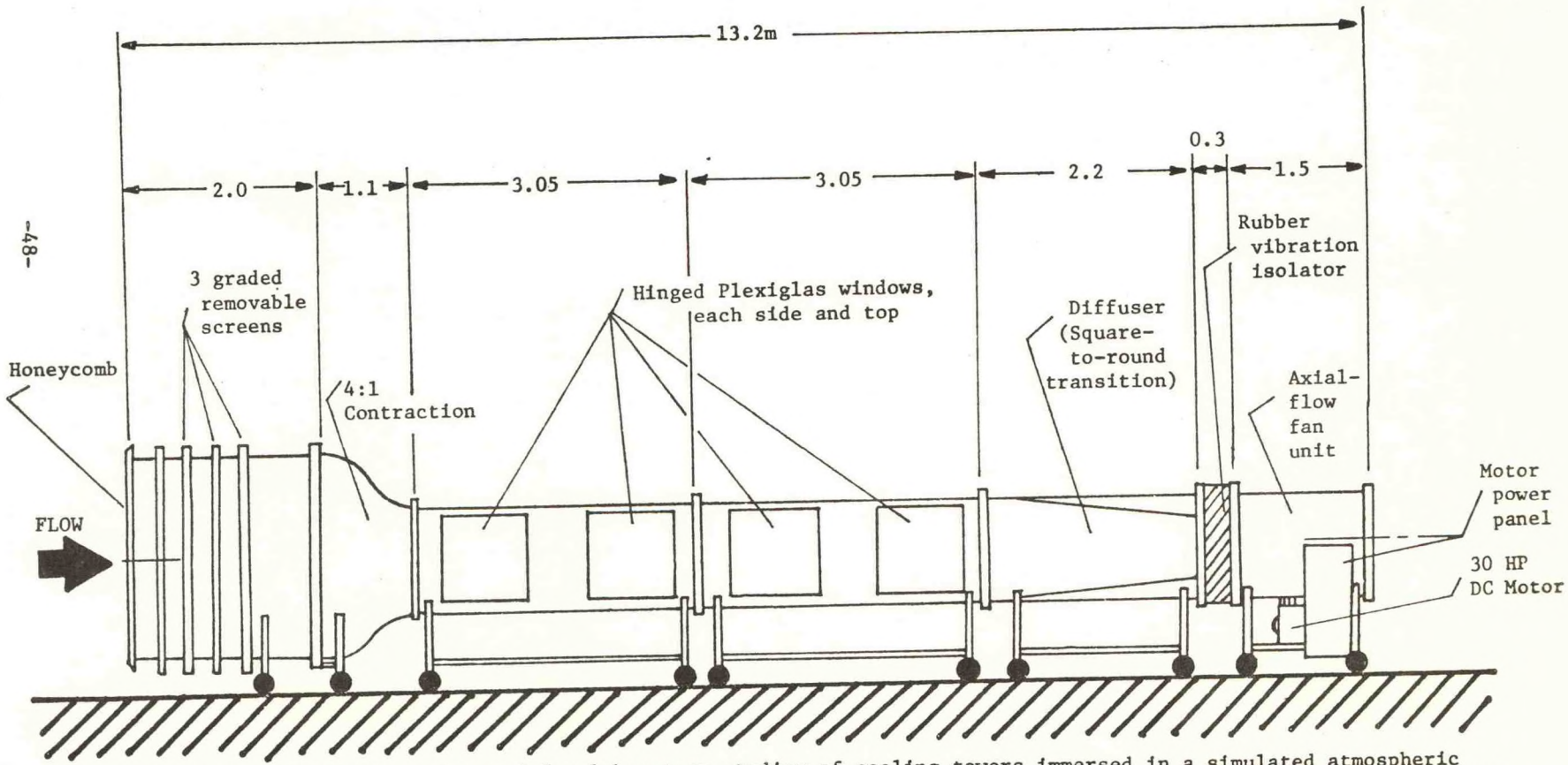


Figure 1: ATDL wind tunnel, to be used for laboratory studies of cooling towers immersed in a simulated atmospheric boundary layer. Test section 1 m. square inside. Flow speed 0-22 m/sec. Modified Wirecomb (Kenney) model 1391.

## 3.3 Additional Equipment

Measurements of flow speed and turbulence levels will be accomplished with standard constant-temperature anemometry techniques. Three channels of linearized Flow Corporation model 750-1 hot wire anemometers are presently on hand; these will probably be supplemented with a Thermo-Systems model 1050 system using hot-film probes for improved ruggedness. At very low flow speeds special techniques such as measuring the eddy-shedding frequency of small cylinders may be necessary; in this method, the velocity is obtained from the known Strouhal number dependence on Reynolds number.

Flow visualization will be accomplished by standard methods including smoke, surface-mounted tufts and flags, grids of tufts, and surface "paints" to reveal eddy structure. A 35 mm motor-driven Canon F-1 camera with a 250 frame film back and several lenses has been purchased; a 16 mm Kodak K-100 movie camera is also available. A small darkroom facility will be set up to permit rapid, on-site processing of exposed film.

Equipment for concentration measurements within the model plumes has not yet been purchased; several of these instruments are under consideration.

The wind tunnel, darkroom, and a model storage area will be housed in a prefabricated steel building 9.1mWx30.5mLx4.3mH. The interior will be temperature-controlled to within ±1°C, and

humidity controlled to ±2% RH. Funds for this building and its HVAC equipment have been provided by ERDA. The building will be located immediately behind the existing ATDL building, within 50m of the ATDL workshop.

# CHAPTER IV

## TENTATIVE SCHEDULE FOR FUTURE WORK

1. Mathematical Modeling of Cooling Tower Plumes

Review of the literature is planned to continue through the end of the present study to insure recent ideas and data are incorporated in the final model. An initial model of cloud growth has already been completed, and is described in Chapter 2, above. Validation of this model against field data will continue until the end of 1976. Work to develop a second generation cloud growth model has already begun; ATDL staff working on this model include S. R. Hanna, C. J. Nappo, and K. S. Rao. Construction of this more sophisticated theory is expected to require about one year. Early validation attempts will begin in about six months, and will aid significantly in developing the model. Final validation will continue until the end of 1977. A sensitivity study of this second-generation plume model will begin in mid-1977, and will continue until the end of the study. Results will be reported in the literature at various stages of the work. The tentative schedule for completion of the various tasks is indicated in Table 16.

2. Physical Modeling of Cooling Towers, Plumes, and Interactions

A preliminary literature survey has been completed; review of the literature will continue until the end of the study to take advantage of newly reported results. Equipment requirements have

been largely compiled and orders placed; virtually all the necessary instrumentation will be either on hand or on order by late fall of 1976. The building to house the wind tunnel should be complete about December 1, 1976. The tunnel will be set up and tested by a factory engineer before final acceptance. A complete check of the wind tunnel's flow behavior and installation of instruments such as probe traversing mechanisms, hot wire probes and recorders, etc. will continue until April, 1977. Efforts to properly simulate neutrally stable atmospheric boundary layer flows will then begin, using the most favorable techniques reported in the literature. Study of individual cooling towers should begin by July, 1977. A range of upwind roughnesses, tower Froude numbers, and tower efflux velocity ratios will be examined. Modifications of tower shape will be considered. Arrays of towers will be studied in 1978; downwash, recirculation, and other interference effects will be treated. ATDL staff engaged in this work will include R. P. Hosker and K. S. Rao. A report summarizing and analyzing the data will be published at the completion of the project. The tentative schedule for these tasks is listed in Table 16.

Other research of interest in evaluating possible weather modification effects of cooling towers will be conducted by G. A. Briggs of ATDL at the U. S. EPA's Fluid Modeling Facility, Research Triangle Park, N. C., from Sept., 1976 to Sept., 1977. Generalized studies are planned of multiple plume merger, the effects of ambient turbulence on strongly buoyant plumes, and the generation and/or concentration

of vorticity near bent-over plumes. The lift-off of an initially wake-entrained buoyant plume will also be examined. The schedule for accomplishment is presently uncertain because of the fairly large number of people expected to be using the EPA facilities during this period, and so has not been listed in Table 16. Results will be reported in the literature.

TABLE 16: Tentative schedule for task accomplishment in study of "Weather Modification Effects of Cooling Towers"

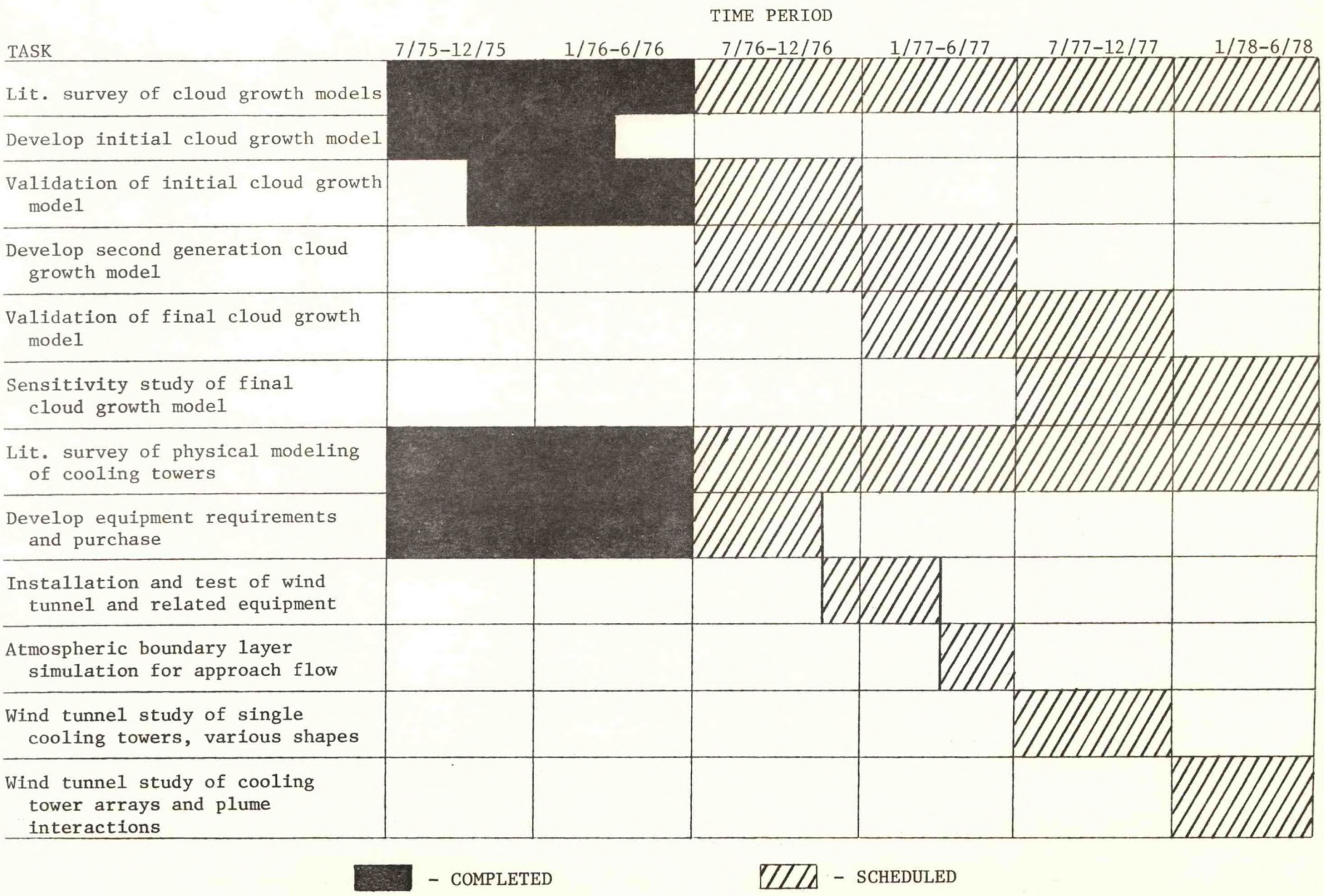

## CHAPTER V

## REFERENCES


Auer, A. H., Jr. (1976) "Observations of an industrial cumulus." J. Appl. Meteorol., 15, 406-413.

Aynsley, E., and Carson J. E. (1973) "Atmospheric effects of water cooling facilities, a summary," presented at the Cooling Tower Institute Annual Meeting, Jan. 29-31, Houston, Tx.

Brennan, P. T., Seymour D. E., Butler M. J., Kramer M. L., Smith M. E., and Frankenburg T. T. (1976) "The observed rise of visible plumes from hyperbolic natural draft cooling towers." Atmos. Environ., 10, no. 6, 425-431.

Briggs, G. A. (1974) "Plume rise from multiple sources," in Cooling Tower Environment-1974, National Technical Information Service, U. S. Department of Commerce, Springfield, Va., 22161, 161-179.

Briggs, G. A. (1974) Discussion following Meyer, et al.'s paper in Cooling Tower Environment-1974, ed. by Hanna and Pell, ERDA-TIC, NTIS CONF-740302, 1975, 352.

Briggs, G. A. (1975) Plume rise predictions. Lectures on Air Pollution and Environmental Impact Analyses. American Meteorol. Soc., 45 Beacon St., Boston, Mass., 59-111.

Brodkey, R. S. (1967) The Phenomena of Fluid Motions (Addison-Wesley Publishing Co., Reading, Massachusetts).

Bugler, T. W., and Tatinclaux J. C. (1974) Scale Effects on Cooling Tower Model Studies, Iowa Institute of Hydraulic Research report no. 168, Univ. of Iowa, September.

Busch, N.E. and Panofsky H. A. (1968) "Recent spectra of atmospheric turbulence," Quart. J. of Roy. Meteor. Soc., 94, no. 400 (April), 132-148.

Campbell, G. S. and Standen N. M. (1969) Progress Report II on Simulation of Earth's Surface Winds by Artificially Thickened Wind Tunnel Boundary Layers, National Aeronautical Establishment tech. rept. LTR-LA-37, National Research Council of Canada, Ottawa, July.

Carson, J. E. (1974) "Meteorological consequences of thermal discharges from nuclear power plants--research needs," in Cooling Tower Environment-1974, ed. by Hanna and Pell, ERDA-TIC, NTIS CONF-740302, 1975, 221-238.

Cermak, J. E., Sandborn V. A., Plate E. J., Binder G. H., Chuang H., Meroney R. N., and Ito S. (1966) Simulation of Atmospheric Motion by Wind Tunnel Flows, Fluid Dynamics and Diffusion Laboratory Tech. Report no. CER66JEC-VAS-EJP-GJB-HC-RNM-SI17, Colorado State University, Ft. Collins, Colorado, May.

Cooling Tower Environment-1974, ERDA Symposium Series, CONF-740302, Nat. Tech. Information Service, U. S. Dept. of Commerce, Springfield, Va., 22161, 638 pp.

Cotton, W. R. (1975) Theoretical cumulus dynamics. Reviews of Geophysics and Space Physics, 13, 419-447.

Counihan, J. (1969) "An improved method of simulating an atmospheric boundary layer in a wind tunnel" Atmospheric Environment 3, no. 2 (March), 197-214.

Counihan, J. (1970) "Further measurements in a simulated atmospheric boundary layer," Atmospheric Environment 4, no. 3 (May), 259-275.

Davenport, A. G. (1963) "The relationship of wind structure to wind loading," in Wind Effects on Buildings and Structures, proceedings of conf. at Nat. Physical Laboratory, Teddington, Middlesex, England, June 26-28 (Her Majesty's Stationery Office, London, 1965), 54-101.

Davenport, A. G. and Isyumov N. (1967) "The application of the Boundary Layer Wind Tunnel to the prediction of wind loading," in Wind Effects on Buildings and structures, proc. of International Research Seminar at the Nat. Research Council, Ottawa, Canada, Sept. 11-15 (Univ. of Toronto Press, 1968), vol. I, 201-225.

Environmental Systems Corporation (1976) Chalk Point Cooling Tower Project Seasonal Test Data for the period December 15-19, 1975, Report no. PPSP-CPCTP-8, Prepared by ESC, Knoxville, Tn. for the Md. Power Plant Siting Program, Chalk Point Cooling Tower Project, 157 pp.

Fletcher, N. H. (1962) The Physics of Rainclouds. Cambridge Univ. Press, London, 386 pp.

Gault, J. D. (1967) Low Altitude Atmospheric Turbulence LO-LOCAT Mid-Term Technical Data Analysis, U.S.A.F. Aeron. Systems Div. Tech. Rept. SEG-TR-67-35, Wright-Patterson AFB, Ohio, August.

Golden, J. (1961) Scale Model Techniques, M. A. thesis, Dept. of Meteor. and Oceanography, New York Univ.

Goldstein, S., editor (1965) Modern Developments in Fluid Dynamics, vols. I and II (Dover Publications, Inc., New York).

Halitsky, J. (1968) "Gas diffusion near buildings," chapter 5-5 in Meteorology and Atomic Energy 1968 (D. H. Slade, ed.), U. S. AEC TID-24190, 221-255.

Halitsky, J., Golden J., Halpern P., and Wu P. (1963) Wind Tunnel Tests of Gas Diffusion from a Leak in the Shell of a Nuclear Power Reactor and from a Nearby Stack, Geophys. Sci. Lab. report 63-2, Dept. of Meteor. and Oceanography, New York Univ.

Hanna, S. R. (1972) "Rise and condensation of large cooling tower plumes." J. Appl. Meteorol., 11, 793-799.

Hanna, S. R. (1974) "Meteorological effects of the mechanical draft cooling towers of the Oak Ridge Gaseous Diffusion Plant," in Cooling Tower Environment-1974, ERDA Symposium Series, CONF-740302, Nat. Tech. Information Service, U. S. Dept. of Commerce, Springfield, Va., 22161, 291-306.

Hanna, S. R. (1976a) "Predicted and observed cooling tower plume rise and visible plume length at the Johne E. Amos power plant." To be published in Atmos. Environ.

Hanna, S. R. (1976b) "Observed and predicted cooling tower plume rise at the John E. Amos power plant, West Virginia," Proceedings of the Third Symposium on Atmospheric Turbulence Diffusion, and Air Quality, American Meteorological Society, Raleigh, North Carolina.

Hanna, S. R. and Gifford F. A. (1975) "Meteorological Effects of Energy Dissipation at Large Power Parks." Bull. Am. Meteorol. Soc., 56, 1069-1076.

Hoult, D. P., O'Dea S. R., Touchton G. L., and Ketterer R. J., (1975) "Turbulent plume in a turbulent cross flow: comparison of wind tunnel tests with field observations," paper #75-49.1 presented at 68th Annual Meeting of the Air Pollution Control Assoc., Boston, Mass., June 15-20.

Hoult, D. P. and Weil J. C. (1972) "Turbulent plume in a laminar cross flow," Atmospheric Environment, 6, no. 8 (August), 513-531.

Isumi, Y., editor (1971) Kansas 1968 Field Program Data Report, USAF Cambridge Research Lab. environmental research paper 379, AFCRL-72-0041, December 27.

Izumi, Y. and Caughey J. S. (1976) Minnesota 1973 Atmospheric Boundary Layer Experiment Data Report, USAF Cambridge Research Lab. environmental research paper 547, AFCRL-TR-76-0038, January 21.

Jones, G. W., Jones, J. W. and Monson K. R. (1969) Interim Analysis of Low Altitude Atmospheric Turbulence (LO-LOCAT) Data, USAF Aeron. Systems Div. Tech. Rept. ASD-TR-69-7, Wright-Patterson AFB, Ohio, February.

Jones, J. W., Mielke R. H., Jones G. W., et al. (1970) Low Altitude Atmospheric Turbulence LO-LOCAT Phase III, USAF Flight Dynamics Laboratory Tech. Rept. AFFDL-TR-70-10, vol. I, part I, Wright-Patterson AFB, Ohio, November.

Kennedy, J. F., and Fordyce H. (1974) "Plume recirculation and interference in mechanical-draft cooling towers," in Cooling Tower Environment-1974, ed. by Hanna and Pell, ERDA-TIC, NTIS CONF-740302, 1975, 58-87.

Kramer, M. L., Seymour D. E., Butler M. J., Kempton R. N., Brennan P. J., Conte J. J. and Thomson R. G. (1975) John E. Amos Cooling Tower Flight Program Data, December 1974-March 1975, by Smith-Singer Meteorologists, Inc., 134 Broadway, Amityville, N.Y., 11701 for American Electric Power Service Corp., P.O. Box 487, Canton, Ohio, 44701.

Kramer, M. L., Smith M. E., Butler M. J., Seymour D. E., and Frankenberg T. T. (1975) "Cooling towers and the environment," paper 75-17.3 presented at the 68th Annual Meeting of the Air Poll. Control Assoc., Boston, Mass., June 15-20.

Landau, L. D., and Lifshitz E. M. (1959) Fluid Mechanics, vol. 6 of Course of Theoretical Physics (Addison-Wesley Publishing Co., Reading, Massachusetts).

Lettau, H. H. (1962) "Theoretical wind spirals in the boundary layer of a barotropic atmosphere," Beiträge zur Physik den Atmosphäre, 35, 195-212.

Lin, J. T., Lin H. T., and Pao Y. H. (1974) Laboratory Simulation of Plume Dispersion in Stably Stratified Flows Over a Complex Terrain, Flow Research, Inc. report no. 29 to the U. S. E.P.A. under contract 68-02-0800, February.

Lloyd, A. (1967) "The generation of shear flow in a wind tunnel," Quart. J. of Roy. Meteor. Soc., 93, no. 395 (January) 79-96.

Ludwig, G. R., Sundaram T. R., and Skinner G. T. (1971) Laboratory Modeling of the Atmospheric Surface Layer with Emphasis on Diffusion, Cornell Aeronautical Laboratory report no. VC-2740-S-2 to the Fallout Studies Branch, Division of BIology and Medicine, U.S. AEC, AEC no. NYO-4038-2, under contract AT(30-1)-4038, July.

Lumley, J. L. and Panofsky H. A. (1964) The Structure of Atmospheric Turbulence (Interscience Publishers, New York).

McVehil, G. E., Ludwig G. R., and Sundaram T. R. (1967) On the Feasibility of Modeling Small Scale Atmospheric Motions, Cornell Aeronautical Laboratory report no. ZB-2328-P-1, April 22.

McVehil, G. E. and Heikes K. E. (1975) Cooling Tower Plume Modeling and Drift Measurement. A Review of the State-of-the-Art, prepared for ASME (Contract G-131-1) by Aerospace Division, Ball Brothers Research Corporation, Boulder, Colorado, 80302.

Meyer, J. H., Eagles T. W., Kohlenstein L. C., Kagan J. A., and Stanbro W. D. (1974) "Mechanical draft cooling tower visible plume behavior: measurements, models, predictions," in Cooling Tower Environment-1974, ERDA Symposium Series, CONF-740302 Nat. Tech. Information Service, U. S. Dept. of Commerce, Springfield, Va., 22161, 307-352.

Monson, K. R., Jones G. W., Mielke R. H., et al., (1969) Low Altitude Atmospheric Turbulence LO-LOCAT Phase III Interim Report, U.S.A.F. Flight Dynamics Laboratory Tech. Rept. AFFDL-TR-69-63, vol. I, Wright-Patterson AFB, Ohio, October.

Nappo, C. J. (1976) "The detailed numerical simulation of vorticity concentration downwind of large heat sources," in ATDL Annual Report to the Atmospheric Effects of Nuclear Energy Centers Program, ATDL-NOAA, Oak Ridge, TN.

Norman, J. M., Thomson D. W., Pena J., and Miller R. (1976) Aircraft Turbulence and Drift Water Measurements in Evaporative Cooling Tower Plumes, Penn. State Univ., Meteorology Dept. research report (draft).

Onishi, Y. and Trent D. S. (1976) Mathematical and Experimental Investigations on Dispersion and Recirculation of Plumes from Dry Cooling Towers at Wyodak Power Plant in Wyoming, Battelle Pacific Northwest Laboratory report BNWL-1982, prepared for ERDA under contract E(45-1):1830, February.

Pasquill, R. (1971) "Wind structure in the atmospheric boundary layer," in A Discussion on Architectural Aerodynamics, Phil. Trans. Roy. Soc. Lond. A. 269, 439-456.

Peterka, J. A. and Cermak J. E. (1974) Simulation of Atmospheric Flows in Short Wind Tunnel Test Sections, Fluid Dynamics and Diffusion Laboratory report CER73-74JAP-JEC32, Colorado State Univ., Ft. Collins, June.

Pope, A and Harper J. J. (1966) Low-Speed Wind Tunnel Testing (John Wiley and Sons, New York).

Rao, K. S. (1976) "3-D subgrid turbulence enclosure models- a critical review," in ATDL Annual Report to the Atmospheric Effects of Nuclear Energy Center Program, ATDL-NOAA, Oak Ridge, Tennessee.

Schlichting, H. (1960) Boundary Layer Theory, 4th Edition, (McGraw Hill Book Company, New York).

Simpson J. and Wiggert V. (1970) "Models of precipitating cumulus towers." Mon. Wea. Rev., 97, 471-489.

Slawson, P. R., Coleman J. H., and Frey J. W. (1974) "Some observations on cooling-tower plume behavior at the Paradise Steam Plant," in Cooling Tower Environment-1974, ERDA Symposium Series, CONF-740302, Nat. Tech. Information Service, U. S. Dept. of Commerce, Springfield, Va., 22161, 147-160.

Snyder, W. H. (1972) "Similarity criteria for the application of fluid models to the study of air pollution meteorology," Boundary-Layer Meteor., 3, no. 1 (Sept.), 113-134.

Sundaram, T. R., Ludwig G. R., and Skinner G. T. (1972) "Modeling of the turbulence structure of the atmospheric surface layer," AIAA Journal 10, no. 6 (June), 743-750.

Sutton, O. G. (1953) Micrometeorology (McGraw-Hill Book Co., New York).

Symes, C. R., and Meroney R. N. (1970) Cone Frustrums in a Shear Layer, Fluid Dynamics and Diffusion Laboratory Tech. Report no. CER70-71CRS-RNM11, Colorado State University, Ft. Collins, Colorado, August.

Templin, R. J. (1969) Interim Progress Note on Simulation of Earth's Surface Winds by Artificially Thickened Wind Tunnel Boundary Layers, National Aeronautical Establishment tech. rept. LTR-LA-22, National Research Council of Canada, Ottawa, February 26.

Townsend, A. A. (1956) The Structure of Turbulent Shear Flow (Cambridge Univ. Press).

Wolf, M. A. (1976a)"Natural draft cooling tower plume characteristics determined with airborne instrumentation." Pac. Northwest Lab. Annual Rep. for 1975 to the USERDA DBER. Part 3 Atmospheric Sciences, BNWL-2000 PT3, 281-288.

Wolf, M. A. (1976b) Private communication dated 10 May 1976.

APPENDIX A

# PREDICTED AND OBSERVED COOLING TOWER PLUME RISE AND VISIBLE PLUME LENGTH AT THE JOHN E. AMOS POWER PLANT

by

Steven R. Hanna

Air Resources
Atmospheric Turbulence and Diffusion Laboratory
National Oceanic and Atmospheric Administration
Oak Ridge, Tennessee 37830

June, 1976

ATDL Contribution File No. 75/21.

## ABSTRACT

A one-dimensional numerical cloud growth model and several empirical models for plume rise and cloud growth are compared with twenty seven sets of observations of cooling tower plumes from the 2900 MW John E. Amos power plant in West Virginia. The three natural draft cooling towers are 200m apart. In a cross wind, the plumes begin to merge at a distance of about 500m downwind. In calm conditions, with reduced entrainment, the plumes often do not merge until heights of 1000m. The average plume rise, 750m, is predicted well by the models, but day-to-day variations are simulated with a correlation coefficient of about .5. Model predictions of visible plume length agree, on the average, with observations for visible plumes of short to moderate length (less than about 1km). The prediction of longer plumes is hampered by our lack of knowledge of plume spreading after the plumes level off. Cloud water concentrations predicted by the numerical model agree with those measured in natural cumulus clouds (about .1g/kg to 1g/kg).

## 1. Introduction

In the assessment of atmospheric effects of energy centers, a crucial problem is the calculation of visible plume and cloud growth caused by emissions from cooling towers. At a power plant, for example, cooling towers emit as much as twice the energy generated for electricity. Typically, more than half of this "waste" energy is in the form of latent heat. Many current power plants use from one to four large natural draft cooling towers, which have the following physical characteristics:

| | |
|---|---|
| top diameter: | ~70m |
| height: | ~150m |
| vertical plume speed: | ~5m/sec |
| difference between plume and ambient T; | ~20°C |

Some power plants use mechanical draft cooling towers, which rely on fans to force the air flow and are not as tall (a typical height is 20 or 30m). Arrays of mechanical draft towers have historically been built in lines, but recent construction includes disc and doughnut shaped systems.

Proposed energy centers, if constructed, will dissipate about 100,000MW of waste heat from a surface area of about $100km^2$. Energy fluxes of this magnitude put energy centers on the same scale as large geophysical phenomena such as bushfires, volcanoes, and thunderstorms (Hanna and Gifford, 1975). Clearly it is very important that we study the possible environmental effects of energy centers before they are built, in order to determine the spacing, tower type, and so on, that will minimize environmental impact.

Unfortunately, the models and observations necessary for these assessments do not exist. The state of art of this area of research is summarized in the conference proceedings entitled Cooling Tower Environment - 1974 and in the critical review by McVehil and Heikes (1975). A few models for estimating visible plume are presented in these publications, but there is very little discussion of cloud growth models. The only published attempts at modeling the cloud physics processes in cooling tower plumes are so-called "one-dimensional models", where plume parameters are a function only of height, as reported by EG&G (1971) and Hanna (1971). In both of these models, Weinstein's (1970) cloud growth model is used as a basis.

In determining the atmospheric effects of energy centers, it is reasonable to begin with simple one dimensional models. Then, after the capabilities of these models are assessed, the research can proceed to two or three dimensional models. The model by Hanna (1971) was revived, encouraged by recent developments in the area of aircraft measurements of cooling tower plumes. For example, M. Wolf (1976), of Battelle Pacific Northwest Laboratory, is using an aircraft-mounted cloud droplet spectrometer to measure water drop characteristics in cooling tower plumes

at the Rancho Seco Plant in California. Norman et al. (1975) of Penn State University are making a nearly complete series of cloud physics and turbulence measurements from their aircraft at the Keystone, Pa., cooling towers. Similar measurements are being made by Woffinden et al. (1976) of Meteorology Research, Inc. as part of the Chalk Point Project.

The observations that are used to test our model were obtained by Kramer et al. (1975) at the John E. Amos, West Virginia, power plant of the American Electric Power Service Corporation. Observations were made on 54 separate occasions during the winter of 1974-1975, aiming for periods when the plume would be as long as possible. Ambient profiles of temperature, dew point, and wind speed were obtained by aircraft; and many photographs of the plume were taken. These measurements are particularly valuable, since in many cases the visible plume obviously extended beyond the point of maximum plume rise, and therefore final plume rise could be obtained. Unfortunately, no in-plume observations were made.

The Amos measurements were analyzed statistically by Brennan et al. (1976), who found very little relationship between plume rise and wind speed, but a good relationship between plume rise and haze layer or inversion height. It is expected that the relationship with haze layer height will deteriorate for measurements made during the warmer seasons of the year, when the haze layer is much deeper.

## 2. Numerical Model Description

The numerical model has been constructed so that it agrees with known relationships for the rise of buoyant stack plumes at small heights and the growth of natural continental cumulus clouds at large heights. It is based on theories of plume rise developed by Briggs (1969), cloud growth developed by Weinstein (1970), and cloud microphysics developed by Kessler (1969). Since the model is one-dimensional (i.e., plume parameters are a function of height only), it cannot be expected to portray cloud growth as well as two or three dimensional models which account for cross-plume gradients. But one-dimensional models have been shown to work quite well for stack plumes and for many cumulus clouds, and are a necessary first step in the analysis of atmospheric effects of energy centers.

The framework of this model was first reported by Hanna (1971), but testing of the model had to wait until sufficient observations of cooling tower plumes were made. A few modifications to the 1971 model were made, based on recent developments in plume rise theory. The first change reflects a suggestion by Briggs (1975) which resolves the paradox that, for a given entrainment rate for bent over plumes, the final plume rise and the rate of change of plume radius with height cannot simultaneously agree with observations. This problem is solved using the knowledge that the rate of

change of the momentum flux with height depends partly on the fact that ambient air above the rising plume must also be accelerated. The effective radius of the "momentum plume" is therefore larger than the radius as determined from temperature differences. Briggs finds that agreement with observations is reached when the following relations are used:

$$\text{For bent over plumes:} \begin{cases} \partial R_m/\partial z = .6 \text{ (momentum plume)} & (1) \\ \partial R_t/\partial z = .4 \text{ (temperature plume)} & (2) \end{cases}$$

where $R_m$ is the radius of the momentum plume and $R_t$ is the radius of the temperature plume. Consequently the ratio, $E_m$, of the effective momentum flux to the momentum flux within the temperature plume approaches $(.6/.4)^2$, or 2.25.

The second modification to the model reflects observations by Slawson et al. (1974) and Meyer et al (1974), that visible plume lengths are consistently underpredicted by basic plume models, due to the fact that inhomogeneities in the plume can result in locally saturated spots, even though the plume is unsaturated on the average. Meyer et al (1974) resolve this problem through the use of a peak factor, explaining that: "it was simply assumed that the excess water-vapor content at the plume center is higher than the average excess water-vapor content predicted in the plume by an empirically

determined constant that is referred to as the peak factor." They suggest that the peak factor equals 1.86. Briggs (1975) has reanalyzed their data and other data, and finds that the peak factor equals 2.0. This factor is incorporated into the present model by assuming that the ratio, $E_w$, of the cross-sectional area of the moisture plume to the temperature plume approaches 1/2. In terms of the rate of change of the radius with height, this assumption can be written:

$$\partial R_w/\partial z = .71\ \partial R_t/\partial z, \qquad (3)$$

where $R_w$ is the radius of the moisture plume. Note that the constant .71 is the inverse of the square root of the peak factor. Equation (3) applies to both vertical and bent over plumes.

The third modification to the model accounts for the stretching of the plume as it rises through layers of wind shear. In order to maintain continuity in the volume flux, the term $(R_t/2U)\ \partial U/\partial z$ is subtracted from the right hand side of equation (1). Since the wind shear is usually positive in the boundary layer, the rate of growth of the plume radius is not as great as it would be in a region of constant wind speed. Murthy (1970) gives solutions to the plume rise equations for a wind profile which satisfies a power law.

The final basic modification to the model is made to account for merging of multiple cooling tower plumes. This states simply that, when the radius of the plume equals one half of the distance between the centers of the towers, the plumes merge and the cross-sectional area of the single merged plume equals the cross-sectional areas of the two or more individual plumes at the time of the merger.

Photographs of the Amos plumes in the report by Kramer et al. (1975) suggest that for bent-over plumes, merger begins at a distance of 300 to 500m downwind. For vertical plumes, where entrainment is less, merger does not begin until heights of 500 to 1000m are reached. It is also interesting that the observed plumes in calm conditions do not constrict, as predicted by plume rise theory, but in all cases steadily increase their radius as height increases. From the plume photographs, it appears that the plume diameter doubles or triples after it rises one tower height (150m).

The following equations are used in the model:

Equation of Motion:

$$\partial(w^2/2)/\partial z=(g/E_m)[(T_p(1 + .61E_wQ_p)-T_e(1 + .61E_wQ_e))/(T_p(1 + .61E_wQ_p)) -E_w(Q_c + Q_h)]-(O_m w^2/R_m) \quad (4)$$

where w(m/s) is the vertical speed, g($m/s^2$) is the acceleration of gravity, T(°K) is temperature, and the Q's (g/g) are specific water densities. The entrainment coefficient for the momentum plume, $O_m$, is defined by $(1/V)dV/dz = O_m/R_m$, where the volume flux, V, equals $UR_m^2$ for a bent over plume and $wR_m^2$ for a vertical plume. Subscripts p, e, c, and h refer to plume variables, environmental variables, cloud water content, and hydrometeor water content, respectively. The term on the left is the vertical acceleration of the plume. The terms on the right are the buoyancy force and the drag or entrainment force.

Equation for Temperature Change:

$$\partial T_p/\partial z = \{-(LE_w/c_p)\partial Q_{ps}/\partial z\}-g/c_p-O(T_p-T_e)/R + \{(L_iE_w/c_p)(Q_h + Q_c)/\Delta z\}$$
$$-\{(LE_w/c_p)O_w(Q_p-Q_e)/R_w\} \quad (5)$$

The terms in curly brackets apply only when the plume is saturated. The subscript s refers to a saturated variable. The parameters L(j/g), $L_i$(j/g), and $c_p$(j/g°K) are the latent heats for vapor-water and water-ice transitions, and the specific heat of air at constant pressure. The entrainment rates O and $O_w$ refer to the temperature and water plumes, respectively. $\Delta z$ is the height increment of the numerical integration. The terms on the right are the heat gained due to condensation, the heat lost due to dry adiabatic expansion, the entrainment rate or heat required to warm entrained air, the heat gained due to freezing of liquid water, and the heat lost as liquid water is evaporated in order to saturate the entrained air. A term suggested by Weinstein (1970) which accounts for the evaporation of liquid water at the plume's edge, was originally included in equation (5). Since the contribution of this term was found to be insignificant, it was removed from the equation.

Equation for Water Vapor Change:

Unsaturated $$\partial Q_p/\partial z = -O_w(Q_p-Q_e)/R_w \quad (6)$$

Saturated $$\partial Q_p/\partial z = \partial Q_{ps}/\partial z \quad (7)$$

In equation (6), for an unsaturated plume, $Q_p$ changes only because of entrainment. In equation (7), for a saturated plume, the loss is due to condensation of liquid water in the rising plume.

Equation for Cloudwater Change:

$$\partial Q_c/\partial z = -\partial Q_{ps}/\partial z - 10^{-3}(Q_c - .0005)/w - .00522 Q_c (1000 Q_h)^{.875}/w - O_w(Q_p + Q_c - Q_e)/R_w \quad (8)$$

The first term on the right hand side is the gain due to condensation in the rising plume. The second and third terms are losses due to conversion and coalescence of cloudwater into hydrometeor water (after Kessler, 1969). The last term is a decrease due to entrainment. Note that cloud water is used first to saturate the entrained air.

Equation for Hydrometeor Water Change:

$$\partial Q_h/\partial z = 10^{-3}(Q_c-.0005)/w + .00522Q_c(1000Q_h)^{.875}/w-4.5Q_h(1000Q_h)^{.125}/(w R_w \cdot \cos(\arctan(w/U)))-O_w Q_h/R_w + K_2/\Delta z \quad (9)$$

Terms one and two are the gains due to conversion and coalescence of cloudwater into hydrometeor water. Term three is the loss due to rainout. Term four is the decrease due to entrainment. The last term ($K_2$) is the saturation deficit of the plume if all of the cloud water has been evaporated into the entrained air after a given height increment, $\Delta z$, but the entrained air is still not saturated. Then if all of the hydrometeor water is evaporated after a given height increment and the entrained air is still not saturated, the whole plume must become unsaturated.

Entrainment:

Vertical Plume:

$$O_m = O = .15 \qquad O_w = .107$$

$$\partial R_m/\partial z = \partial R/\partial z = .15-R(g/T_p)(T_p-T_e)/2w^2$$

$$\partial R_w/\partial z = .71\partial R/\partial z \quad (10)$$

Bent Over Plume:

$$O_w = .57 \qquad O = .8 \qquad O_m = 1.2$$

$$\partial R/\partial z = .4-(R/2U)\partial U/\partial z \quad (11)$$

$$\partial R_w/\partial z = .71\partial R/\partial z$$

$$\partial R_m/\partial z = 1.5\partial R/\partial z$$

The entrainment relations are based on Briggs (1975) latest guidelines. They are in rough agreement with Cotton's (1975) review of entrainment rates used in cumulus cloud models. He finds that various investigators use entrainment coefficients, 0, ranging from zero to unity, depending on which value gives predicted cloud heights in agreement with a particular set of observations.

The entrainment formulas for bent over plumes are used when the local wind speed, U, exceeds 1 m/s. Consequently, the entrainment constants may switch from those appropriate for bent over plumes to those appropriate for vertical plumes at different heights in the same run.

Saturation Specific Humidity:

a) $T_1 = 273.16°K<T<373°K$

$$\ln Q_{ps} = 2.303(10.79574(1-T_1/T) + 1.50475\times10^{-4}(1-10^{-8.2969(T/T_1-1)}) + .42873\times10^{-3}(10^{4.76955(1-T_1/T)}-1)) - 5.028 \ln T/T_1 - \ln p + 1.335 \quad (12)$$

b) $T<T_1 = 273.16°K$

$$\ln Q_{ps} = 2.303(-9.09685(T_1/T-1) + .87682(1-T/T_1)) - 3.56654 \ln T_1/T - \ln p + 1.335 \quad (13)$$

where p is pressure in millibars, calculated by means of the hydrostatic equation. These two empirical equations are the "Goff-Gratch" formulas, as given by the World Meteorological Organization (1966). Any equation relating T and $Q_{ps}$, such as the Clausius-Clapeyron equation, could be used in place of equations (12) and (13).

Equations (12) and (13) are plotted in Figure 1, for p = 1000mb, forming the psychrometric curve which is the basis of several published methods for determining the vapor content and temperature of plumes (e.g., Wigley and Slawson, 1971). The technique is illustrated by plotting the initial saturated plume position $(T_{po},Q_{po})$ and the unsaturated environment position $(T_e,Q_e)$. Depending on the relative amounts of plume air and environment air in the resulting mixture, the rising plume can be predicted to be somewhere along the line between these two points. However, if the resulting mixing ratio, $Q_{pl}$, is greater than the saturation mixing ratio, $Q_{pls}(T_{pl})$, then some of the water vapor must condense, and the actual position $(T'_{pl},Q'_{pl})$ is approached. The slope of the dotted line, $\Delta Q/\Delta T$, or $L/c_p$, equals -.8 on this figure. If there were no initial liquid water, then the concentration of liquid water at position $(T'_{pl},Q'_{pl})$ would be $(Q_{pl}-Q'_{pl})$. The end of the visible plume is the point at which the straight line crosses the curved line near the bottom of figure 1.

Unfortunately, the psychrometric technique is not so handy for plumes from natural draft cooling towers, which rise several hundred meters. The saturation curve shifts as height (i.e., pressure) changes. Furthermore, the environmental position ($T_e$, $Q_e$) may vary considerably over the depth of the plume. It is still possible to use the psychrometric chart for a well-mixed adiabatic environment (see Briggs, 1975) where the straight line in Figure 1 can be shifted uniformly to the left by the amount $zg/c_p$ in order to account for temperature changes with height. The psychrometric chart technique has been applied most successfully to short plumes from mechanical draft cooling towers (see McVehil and Heikes, 1975).

Equations (1) through (13) are a complete set, and are solved on a high-speed digital computer using height steps of .01m, .1m, and 1m for heights less than 10m, between 10 and 100m, and above 100m, respectively. As may be expected, the possibility of a phase change requires detailed logical steps in the computer program. For example, if the calculated vapor content $Q_p$ happens to be greater than the saturated vapor content $Q_{ps}$ after a single height step is taken, it is necessary to condense some of the excess vapor. The condensation takes place in such a way that the energy released by condensation just balances the heat gained due to a temperature increase.

Several of the parameterizations in this model are based on measurements in natural clouds rather than cooling tower clouds. For example, rainout is included in the program (eq. 9, term 3), using a mechanism suggested by Simpson and Wiggert (1969). This mechanism is based on the assumption that the relative rate of loss of hydrometeor water in a given time interval is proportional to the distance that the water drops would fall in that interval, divided by the vertical component of the plume radius. Because this relation was first developed for large cumulus clouds, it is questionable whether the rainfall rates that it yields in our application are realistic. Unfortunately, there are not yet sufficient observations in cooling tower plumes to derive empirical relationships for cloud physics proeesses. Some of this information is beginning to come from the Penn State program (Norman et al, 1975), but much more needs to be done.

3. Input Data

All of the observation periods were during the winter of 1974-1975, and were deliberately chosen by Kramer et al (1975) so that a long visible plume would be present. Low temperatures, high relative humidities, low wind speeds and stable conditions all increase the chances of a long visible plume. The first two conditions lower the saturation deficit (saturated water vapor content minus actual water vapor content, or $(Q_{es}-Q_e)$) of the ambient air, while the last two conditions increase the concentration of excess water in the plume. During a run, the aircraft would obtain vertical profiles of dry bulb temperature, dew point, and wind speed in the lowest 2000m. Several photographs of the plume were taken, and the visible plume height and length were noted. At the same time, power plant personnel provided information on the net load of the three cooling towers. These data have been summarized in a very complete fashion, including drawings of the visible plume, by Kramer et al (1975). About half of the runs could not be used in this study, because of problems such as the disappearence of the plume in a cloud deck or insufficient ambient profile data. Of the 27 runs which are analyzed, seven have bent over plumes in which the visible plume does not extend to the point

of maximum plume rise, seven have vertical plumes, and 13 have bent over plumes in which the visible plume does extend to the point of maximum plume rise.

The three cooling towers at the Amos plant have the characteristics listed in Table 1.

Table 1

Specifications for Amos Cooling Towers (from Kramer et al (1975)

| | height | top radius | $w_o$ | Capacity |
|---|---|---|---|---|
| Towers 1 & 2 | 132m | 29m | 4.6m/s | 800MW(each) |
| Tower 3 | 150m | 40m | 4.2m/s | 1300MW |

The towers are in a line, spaced 200m apart. During the observation periods, the plant ran close to its generating capacity of 2900MW. The initial heat flux used in the model is modified based on the actual energy output for each observation period. Also, prior to plume merger (which is assumed to occur when plume radius equals ½ tower spacing, or 100m), only the plume from tower 3 is modeled. The initial plume radius, $R_o$, is taken as 40m, and the initial plume vertical speed, $w_o$, is assumed to be 4.4m/s (the average over the towers).

The initial plume temperature is estimated by an empirical relation derived from the specifications in Kramer et al. (1975):

$$T_{po} = (297.4 + .635(T_d - 273))(1 + .01(1-RH)), \qquad (14)$$

where $T_d$ and RH are the ambient dew point and relative humidity. Since the Amos plant does not always operate at full capacity, the ratio of actual to full power is also input for each run. This ratio is used to revise the plume temperature calculated by equation (14) by assuming that the actual difference between the plume and environment temperatures equals the power ratio times the temperature difference calculated using equation (14). These assumptions were not tested, since no measurements of initial plume temperature were made at the Amos plant.

To insure continuity of the momentum flux, the effective initial plume radius for bent over plumes is calculated from the equation (Hanna, 1972):

$$R_{eff} = R_o(w_o/U)^{1/2} \qquad (15)$$

The mixing ratio of the initial cloud water, $Q_c$, and hydrometeor water, $Q_h$, are also required as input to the model. Both have arbitrarily been set equal to .001, on the basis that fog or cloud is obviously present at the tower mouth; and the sum of the two, .002g/g, is typical for vigorous natural cumulus clouds (Fletcher, 1962). If the plume evaporates, however, buoyancy will be reduced slightly due to the energy that must be taken from the air to evaporate the liquid drops. For example, if the initial liquid water content, .002g/g, were to evaporate at the tower mouth, plume temperature would be reduced by $(L/c_p)(.002g/g)$, or 5°C.

Because of the possibility that errors would be introduced by the arbitrary specification of $Q_c$ and $Q_h$, a sensitivity test was run in which $Q_c$ (which equals $Q_h$) was set equal to .00001, .0001, .001, and .01 g/g. It was found that, when the visible plume is large and a cloud forms in its upper reaches, the initial values of $Q_c$ and $Q_h$ have little effect on final plume rise and cloud water concentration. But for dry ambient conditions when the plume evaporates at a height of about 50m, the initial values of $Q_c$ and $Q_h$ can have a significant effect on plume length and plume rise. The results of running the model for an isothermal ambient atmosphere (10°C) with 50% relative humidity are given in Table 2.

Table 2

Model Output for Isothermal Atmosphere (10°C)

with 50% RH and U = 10m/s.

| Initial $Q_h$ and $Q_c$ (g/g) | Plume Rise (m) | Visible Plume Height (m) | Visible Plume Length (m) | $Q_c$ at max | z(m) |
|---|---|---|---|---|---|
| .00001 | 249 | 52 | 165 | .00057 | 15 |
| .0001 | 248 | 52 | 165 | .00063 | 15 |
| .001 | 232 | 67 | 230 | .00129 | 10 |
| .01 | 138 | 138 | 610 | .01000 | 0 |

It is seen from this table that when the initial $Q_c$ equals $10^{-5}$ or $10^{-4}$, plume parameters are not significantly affected. But when $Q_c$ equals $10^{-3}$, the value used in analyzing the Amos data, plume rise decreases by 7% and visible plume height increases by 29% above that for plumes which begin with essentially no liquid water. When $Q_c$ equals $10^{-2}$, which is a concentration at least an order of magnitude greater than that observed in natural clouds, plume rise is nearly halved and the plume is visible through its point of maximum rise. It can be concluded that the possibility of errors in our choice of initial $Q_h$ and $Q_c$ introduces an uncertainty of about 10 to 20% in calculations of visible plume length for plumes on dry days, but has little effect for plumes on humid or cold days, when the initial liquid water never has a chance to evaporate.

There is not room here to include all of the 27 sets of Amos data used in this analysis. But as an example of the input data, the observations by Kramer et al. (1975) during run 6 are listed in Table 3. These data were used to generate the output in Figure 2, which is discussed in a later section.

Table 3

Observations at John E. Amos power plant (Kramer et al., 1975), for 18 Dec. 1974 (Run 6).

| Height Above Tower (m) | Ambient Dry Bulb °K | Ambient Dew Point °K | Wind Speed m/s |
|---|---|---|---|
| 0 | 268.0 | 266.9 | |
| 122 | 266.9 | 266.9 | 9 |
| 243 | 265.2 | 265.2 | |
| 365 | 264.1 | 264.1 | |
| 426 | 263.6 | 263.6 | |
| 578 | 263.0 | 263.0 | |
| 700 | 262.4 | 262.4 | |
| 821 | 261.9 | 261.9 | |
| 942 | 260.8 | 260.8 | |
| 1064 | 259.7 | 259.7 | |
| 1186 | 259.1 | 259.1 | 12 |

Ratio of actual power to maximum power = .83
Initial plume temperature (from equation 14) = 290°K
Observed plume rise = 850m
Observed visible plume length = 9.6km

## 4. Results

The computer model was run for each of the 27 test cases, and values of total plume rise and visible plume height and length were noted. Also, some simple formulas for estimating plume rise and visible plume parameters were tested.

### 4.1 Final plume rise

In nineteen of the observation periods analyzed, the visible plume extends through the point of maximum plume rise. The average wind speed and vertical potential temperature gradient through the layer in which plume rise took place are given in Table 4. In addition, the saturation deficit in the ambient air at the tower top is given. The observed plume rise listed in the table refers to the final equilibrium height of the plume centerline. All heights are in meters above the tower top.

In column five of the table, the height of the base of the lowest significant inversion in the temperature sounding is given. This height might also be called the mixing height. For the observations when an inversion is present, the average inversion height is 820m and the average observed plume height is 790m. The correlation coefficient between inversion height and observed plume height is .90. This good agreement has led Brennan et al. (1976),

## Table 4

### Observed and Calculated Plume Rise

| Run | $\bar{U}$ (m/s) | Ambient tower top saturation deficit (g/kg) | $\Delta\theta/\Delta Z$ over depth of plume (°C/mx$10^3$) | Inversion height above tower (m) | Observed plume rise (m) | Model plume rise (m) | Analytical Plume rise: sensible one unit (m) | Analytical Plume rise: sensible + latent all units (m) | $E_N$ applied to sensible one unit (m) |
|---|---|---|---|---|---|---|---|---|---|
| 1 | 14 | .43 | 13.5 | | 560 | 260 | 250 | 450 | 270 |
| 6 | 11 | .13 | 3.0 | | 850 | 820 | 430 | 770 | 490 |
| 8a | 9 | 0 | 9.8 | | 370 | 350 | 250 | 450 | 270 |
| 10a | 5 | .60 | 2.1 | 720 | 820 | 820 | 590 | 1060 | 700 |
| 11 | 0 | 1.34 | 6.1 | 660 | 880 | 900 | 980 | 1500 | |
| 12 | 6 | 1.25 | 1.2 | 1140 | 1060 | 1200 | 720 | 1280 | 870 |
| 15 | 3 | .28 | 10.7 | | 1120 | 790 | 780 | 1200 | |
| 16 | 6 | .41 | 7.2 | 1200 | 1160 | 700 | 380 | 680 | 430 |
| 17a | 8 | .29 | 6.7 | 360 | 360 | 430 | 410 | 730 | 460 |
| 18 | 6 | .78 | 5.6 | | 910 | 720 | 410 | 730 | 460 |
| 19 | 0 | 1.07 | 6.9 | 840 | 800 | 970 | 910 | 1400 | |
| 24 | 6 | .60 | 4.0 | 750 | 760 | 630 | 500 | 900 | 580 |
| 28a | 5 | .52 | 21.8 | | 360 | 400 | 310 | 570 | 340 |
| 31 | 0 | 1.02 | 11.6 | | 500 | 900 | 780 | 1200 | |
| 35a | 3 | .87 | 9.8 | 390 | 360 | 590 | 480 | 880 | 550 |
| 44 | 8 | 1.16 | 1.9 | 960 | 910 | 420 | 510 | 910 | 590 |
| 45 | 7 | 1.16 | 5.6 | 1200 | 910 | 370 | 390 | 700 | 440 |
| 47 | 0 | 1.44 | 3.8 | 900 | 800 | 1020 | 910 | 1400 | |
| 48a | 7 | 1.46 | 7.6 | 750 | 670 | 360 | 340 | 610 | 380 |
| Avg. | 5.6 | .76 | 7.4 | 820 | 750 | 670 | 540 | 920 | |

in an independent assessment of these observations, to conclude that, when an inversion lid is present, the plume will rise to this lid and stop. The inversion lids are formed by the natural buoyant and mechanical mixing actions in the boundary layer. Apparently the energy fluxes in the cooling tower plumes are similar to those in natural convective elements during the winter in West Virginia, and the plumes, like the natural convective elements, rise to the base of the inversion lid. But since these inversion layers are often shallow and weak, it is difficult to measure them accurately with the aircraft probe. Consequently, the detailed structure of the inversion lid cannot be included in the numerical plume and cloud growth model. During the summer, when the height of the inversion layer is greatly increased due to the increased surface heat fluxes, the cooling tower plume is less likely to reach the top of the mixed layer.

The output of a typical computer run is given in Figure 2, based on the input data in Table 3. A slight change in curvature of the predicted $\Delta T$, w, and $Q_c$ profiles is evident at a height of about 200m. This is the height at which the three plumes merge in this run, and the buoyancy flux increases by

a factor of about 2.3. Since the ambient atmosphere in this run is nearly saturated pseudoadiabatic, the plume rises quite high and contains a moderate amount of cloud water through its entire trajectory.

The estimates of plume rise from the numerical model for each run are in column 7 of Table 4. The difference between average observed (750m) and estimated (670m) plume rise is about 12%. The correlation coefficient is .49, which can be considered fair. The observed and predicted plume rises are plotted in Figure 3.

Maximum cloud water concentration, $Q_c$, predicted by the numerical model ranges from .0010 to .0016 g/g, in agreement with typical values reported by Fletcher (1962) for natural cumulus clouds. Unfortunately, the aircraft did not obtain any measurements of liquid water concentrations for comparison with these predictions.

The last three columns in Table 4 contain analytical estimates of plume rise. The formulas suggested by Briggs (1969)

for plume rise, H, are used:

$$H = 5.0F^{1/4}s^{-3/8} \qquad \text{Vertical} \qquad (16)$$

$$H = 2.9(F/Us)^{1/3} \qquad \text{Bent-over} \qquad (17)$$

where the buoyancy flux, F, and stability parameter, s, are defined by the relations:

$$F = w_o R_o^2 (g/T_{vpo})(T_{vpo} - T_{veo}) \qquad (18)$$

$$s = (g/T_{eo})(\partial\theta_e/\partial z) \qquad (19)$$

In these relations the subscript v refers to virtual temperature. If the sensible heat from a single tower unit is used in estimating the buoyancy flux, F, then the estimated plume rises in column 8 of Table 4 are obtained. The average estimated plume rise is 540m, or 28% lower than observed. The correlation coefficient between estimated and observed plume rise is .37. One reason for this low correlation is that average temperature gradients are used in calculating the stability parameter, s. The effects of small inversion layers are smoothed out by the analytic technique, but have a great influence on the observed plumes.

Note that the correlation between estimates of the analytical and numerical models is .82. In otherwords, the numerical model is not much different from or better than the simple analytical model for estimating plume rise.

Another estimate of plume rise can be obtained by redefining the buoyancy parameter to include the latent heat (Hanna, 1972):

$$F = w_o R_o^2 g[(T_{vpo}-T_{veo})/T_{vpo} + (L/c_p T_{vp})(Q_{po}-Q_{eo})] \qquad (20)$$

If the sensible plus latent fluxes from the three cooling towers are added together to form F, the predictions are obtained which are listed in column 9 of Table 4. The average plume rise using the maximum F is 920m, or 23% greater than observed. Clearly the actual effective buoyancy flux is somewhere between the sensible flux from a single tower and the total heat fluxes from all towers.

The empirical technique suggested by Briggs (1974) for estimating the plume rise from multiple sources was also applied, and the results are in the last column of Table 4. He derived his formula from observations of plume rise from multiple stacks at TVA power plants. The plume rise from N stacks equals the plume rise from a single stack, H, multiplied by an enhancement factor, $E_N$, defined by:

$$E_N = ((N + S)/(1 + S))^{1/3}$$

where $$S = ((N-1)\,\Delta x/N^{1/3}H)^{3/2}$$

The distance $\Delta x$ is the spacing between towers, which equals 200m at Amos. It is seen from the last column of Table 4 that the enhancement factor for these data, assuming that H is the plume rise due to sensible heat only from a single tower, ranges from 1.08 to 1.21. This additional rise brings the magnitudes of the plume rise estimates closer to the observations, but does not increase the correlation coefficient.

4.2 Visible plume dimensions

In addition to the runs analyzed above, there were also seven runs in which the visible plume was moderately long but did not extend through the point of maximum plume rise. Since visible plume length is not well defined for plumes occurring in calm conditions, analysis will be limited to the bent over cases. Observed visible plume lengths are obtained using the photographs published by Kramer et al. (1975) for the short plumes in Table 5, and from aircraft observers' notes supplied by Conte (private letter, 1975) for the longer plumes in Table 6. The aircraft observers' notes were not used for the shorter plumes because the accuracy of the visible plume length listed by the aircraft observers is ±¼ mile.

Table 5

Visible Plume Dimensions for Plumes whose Visible Portion

does not Reach the Point of Maximum Rise

| Run | $\bar{U}$ (m/s) | ambient saturation deficit (g/Kg) | | observed | | numerical model | | analytical model | | ambient RH at plume level |
|---|---|---|---|---|---|---|---|---|---|---|
| | | tower top | plume level | visible plume height (m) | visible plume length (m) | visible plume height (m) | visible plume length (m) | visible plume height (m) | visible plume length (m) | |
| 2 | 13 | 3.0 | 3.9 | 100 | 200 | 75 | 290 | 100 | 370 | .4 |
| 3 | 10 | 2.6 | 2.7 | 150 | 500 | 120 | 350 | 140 | 400 | .65 |
| 13 | 10 | .86 | 1.8 | 100 | 300 | 150 | 480 | 210 | 730 | .6 |
| 20 | 10 | 2.8 | 3.9 | 200 | 400 | 70 | 250 | 120 | 290 | .45 |
| 27 | 20 | 1.5 | 2.0 | 390 | 600 | 120 | 450 | 110 | 800 | .55 |
| 39 | 15 | 2.9 | 3.6 | 240 | 450 | 140 | 240 | 100 | 430 | .45 |
| 41 | 16 | 3.5 | 3.2 | 50 | 300 | 55 | 290 | 80 | 360 | .35 |
| Avg. | 13 | 2.5 | 3.0 | 180 | 390 | 100 | 340 | 120 | 450 | .50 |

Table 6

Visible Plume Dimensions for Plumes where the Visible Plume Extends through the Point of Maximum Rise

| Run | $\bar{U}$ (m/s) | ambient tower top saturation deficit g/kg | saturation deficit at plume elev. g/kg | observed visible plume length (m) | ambient RH at plume level |
|---|---|---|---|---|---|
| 1 | 14 | .43 | 2.2 | 1600 | .4 |
| 6 | 11 | .13 | 0 | 9600 | 1. |
| 8a | 9 | 0 | .65 | 4800 | .9 |
| 10a | 5 | .60 | 0 | 25600 | 1. |
| 12 | 6 | 1.2 | 0 | 4800+ | 1. |
| 16 | 6 | .41 | 1.3 | 2400 | .8 |
| 17a | 8 | .29 | .29 | 8000 | .9 |
| 18 | 6 | .78 | 1.1 | 1600 | .7 |
| 21 | 9 | .43 | 1.8 | 1600 | .6 |
| 24 | 6 | .60 | .55 | 16000+ | .85 |
| 44 | 8 | 1.2 | .29 | 9000 | .9 |
| 45 | 7 | 1.2 | 1.5 | 1600 | .6 |
| 48a | 7 | 1.5 | 1.2 | 32000+ | .8 |
| Avg. | 8 | .67 | .84 | 4800m (median) | .80 |

In Table 5 the observed relative humidity, wind speed, visible plume height and length, and ambient saturation deficits at tower top and plume height are given for the set of plumes of moderate length. The average visible plume height and length predicted by the numerical model are seen to agree with the average of the observations fairly well. But the correlation between variations in observed and predicted lengths is poor. This poor correlation can be explained by the fact that weather conditions (U, T, $\Delta Q$, RH) are quite similar for each of the runs in Table 5, and consequently we are dealing with comparatively small differences among fairly large numbers. It can be concluded that, for wind speeds of about 13 m/s and saturation deficits of about 3g/kg, visible plume length at the Amos Plant is about 400m.

The results of a simple analytical model suggested by Hanna (1974) are given in columns nine and ten of Table 5. Formulas for visible plume height, h, and length, $\ell$, of bent over plumes are based in this model on the hypothesis that the tip of the visible plume occurs when the initial flux of excess water, $V_o Q_{po}$, in the plume just balances the saturation deficit flux, $V(Q_{eos}-Q_{eo})$:

$$h = 2R_o(w_o/U)^{1/2}[(2Q_{po}/(Q_{eos}-Q_{eo}))^{1/2}-1] \qquad (23)$$

$$\ell = 1.4(R_o^{3/2}U^{3/4}w_o^{3/4}/F^{1/2})[(2Q_{po}/Q_{eos}-Q_{eo}))^{1/2}-1]^{3/2} \qquad (24)$$

Note the occurrence of the peak factor, set equal to 2, inside the brackets of these equations. As expected, the analytical predictions of h and $\ell$ agree fairly well with the predictions of the numerical model, but offer no significant improvement in accounting for the variability of the observed parameters.

Observations and predictions for the longer plumes are in Table 6. Note that for these longer plumes, extending beyond the point of maximum plume rise, average saturation deficit has dropped to .7 g/kg, average wind speed has dropped to 8 m/s, and average relative humidity increased to 80%, when compared with the shorter plumes in Table 5. The plus sign after three of the observed visible plume lengths indicates that the plume merged with existing clouds at that distance.

In Figure 4, observed plume length is plotted versus (1-RH) for all the observations in Tables 5 and 6. The ambient relative humidity at plume height is used for RH. The correlation coefficient is -.58 for these data. The line on the figure is given by the formula

$$\ell = (2.15 \times 10^4 m) e^{-7.6(1-RH)} \qquad (25)$$

and is valid only for the Amos location during the winter. During the summer, when a given relative humidity implies a much larger saturation deficit, the line in Figure 4 can be expected to shift downwards considerable.

It is expected that the chances for a long plume would increase as wind speed, U, decreases and as saturation deficit, $Q_{es}-Q_e$, decreases. This relationship is tested in Figure 5, where observed plume length is plotted versus $U(Q_{es}-Q_e)$. The saturation deficit is measured at plume level. If the data followed by a + are not included, then the correlation coefficient is -.51.

The analytical model, equation (24), was not applied to the data in Table 6 because there is no information available on the increase in radius of cooling tower plumes after they have leveled off. Gifford (1975) reports TVA data on the observed spread of stack plumes, but they have a much smaller initial size and less plume rise than cooling tower plumes. Since most of the Amos plumes analyzed here terminate in stable layers, the passive diffusion should be very slight. This question cannot be satisfactorily resolved until further measurements are made.

## 6. Acknowledgements

This work was performed under an agreement between the National Oceanic and Atmospheric Administration and the Energy Research and Development Administration. Discussions with G. A. Briggs were very helpful. I would not have been able to obtain the observations so quickly without the assistance of M. E. Smith, P. T. Brennan, M. L. Kramer, and J. J. Conte of Smith-Singer Meteorologists, Inc. and D. L. Mazzitti of the American Electric Power Service Corporation. V. Quinn of the Air Resources Laboratory in Las Vegas contributed many valuable suggestions in his review of this manuscript.

## REFERENCES


Brennan P. T., Seymour D.E., Butler M.J., Kramer M. L., Smith M.E., and Frankenburg T. T. (1976) The observed rise of visible plumes from hyperbolic natural draft cooling towers. Atmos. Environ., in press.

Briggs G. A. (1969) Plume Rise. AEC Critical Review Series, TID-25075 from Clearinghouse for Fed. Scient. and Tech. Inf., U.S. Dept. of Comm., Springfield, Va., 82 pp.

Briggs G. A. (1974) Plume rise from multiple sources, in Cooling Tower Environment-1974, National Technical Information Service, U. S. Department of Commerce, Springfield, VA., 22161, 161-179.

Briggs G. A. (1975) Plume rise predictions. Lectures on Air Pollution and Environmental Impact Analyses. American Meteorol. Soc., 45 Beacon St., Boston, Mass., 59-111.

Cooling Tower Environment-1974, ERDA Symposium Series, CONF-740302, Nat. Tech. Information Service, U. S. Dept. of Commerce, Springfield, Va., 22161, ($13.60), 638 pp.

Cotton W. R. (1975) Theoretical cumulus dynamics. Reviews of Geophysics and Space Physics, 13, 419-447.

E. G. & G., Inc. (1971) Potential environmental modifications produced by large evaporative cooling towers, prepared for Water Quality Office, EPA, Cont. no. 14-12-542 by E. G. & G. Environmental Services Operation, Boulder, Colo., 75 pp.

Fletcher N. H. (1962) The Physics of Rainclouds. Cambridge Univ. Press, London, 386 pp.

Gifford F. A. (1975) Turbulent diffusion typing schemes: a review. Nuclear Safety, 17, 68-86.

Hanna S. R. (1971) Meteorological effects of cooling tower plumes. presented at Cooling Tower Inst. Meeting, Houston, 25 Jan., 17 pp., available as report no. 48 from ATDL, P.O. Box E, Oak Ridge, Tenn., 37830.

Hanna S. R. (1972) Rise and condensation of large cooling tower plumes. J. Appl. Meteorol., 11, 793-799.

Hanna S. R. (1974) Meteorological effects of the mechanical draft cooling towers of the Oak Ridge Gaseous Diffusion Plant, in Cooling Tower Environment-1974, ERDA Symposium Series, CONF-740302, Nat. Tech. Information Service, U.S. Dept. of Commerce, Springfield, Va., 22161, ($13.60), pp 291-306.

Hanna S. R. and Gifford F. A. (1975) Meteorological Effects of Energy Dissipation at Large Power Parks. Bull. Am. Meteorol. Soc., 56, 1069-1076.

Kessler E. (1969) On the Distribution and Continuity of Water Substance in Atmospheric Circulations Meteorol. Monographs, 10, 84 + ixpp, published by the Am. Meteorol. Soc, 45 Beacon St., Boston.

Kramer M.L., Seymour D. E., Butler M. J., Kempton R. N., Brennan P. J., Conte J. J. and Thomson R. G. (1975) John E. Amos Cooling Tower Flight Program Data, December 1974-March 1975, by Smith-Singer Meteorologists, Inc., 134 Broadway, Amityville, N.Y., 11701 for American Electric Power Service Corp., P.O. Box 487, Canton, Ohio, 44701.

McVehil G. E. and Heikes K. E. (1975) Cooling Tower Plume Modeling and Drift Measurement. A Review of the State-of-the-Art, prepared for ASME (Contract G-131-1) by Aerospace Division, Ball Brothers Research Corporation, Boulder, Colorado, 80302.

Meyer J. H., Eagles T. W., Kohlenstein L. C., Kagan J. A., and Stanbro W. D. (1974) Mechanical draft cooling tower visible plume behavior: measurements, models, predictions, in Cooling Tower Environment-1974, ERDA Symposium Series, CONF-740302 Nat. Tech. Information Service, U. S. Dept. of Commerce, Springfield, Va., 22161, ($13.60), 307-352.

Murthy C. R. (1970) On the mean path of a buoyant chimney plume in non-uniform wind. J. Appl. Meteorol., 9, 603-611.

Norman J. M., Thomson D. W., Pena J., and Miller R. (1975) Aircraft turbulence and drift water measurements in evaporative cooling tower plumes. Dept. of Meteorol., Penn. State Univ., University Park, PA., 16802.

Simpson J. and Wiggert V. (1970) Models of precipitating cumulus towers. Mon. Wea. Rev., 97, 471-489.

Slawson P. R., Coleman J. H., and Frey J. W. (1974) Some observations on cooling-tower plume behavior at the Paradise Steam Plant, in Cooling Tower Environment-1974, ERDA Symposium Series, CONF-740302, Nat. Tech. Information Service, U.S. Dept. of Commerce, Springfield, Va., 22161, ($13.60), 147-160.

Wigley T.M.L. and Slawson P. R. (1971) On the condensation of buoyant, moist, bent-over plumes. J. Appl. Meteorol., 10, 259-263.

Weinstein A. I. (1970) A numerical model of cumulus dynamics and microphysics. J. Atmos. Sci., 27, 246-255.

Woffinden, G. J., Anderson, J. A., and Harrison, P. R. (1976) Aircraft Survey, Chalk Point Cooling Tower Plume, Dec. 1975, Rept. no. 76R-1910 by MRI, Altadena, Calif. 91001 for the Md. Power Plant Siting Program. 32 pp + appendices.

Wolf, M. A., (1976) Natural draft cooling tower plume characteristics determined with airborne instrumentation. Pac. Northwest Lab. Annual Rep. for 1975 to the USERDA DBER. Part 3 Atmospheric Sciences, BNWL-2000 PT3, 281-288.

World Meteorol. Org., 1966: International Meteorological Tables, WMO-188-TP-94, introd. to tables 4.6 and 4.7.

## APPENDIX B

# OBSERVED AND PREDICTED COOLING TOWER PLUME RISE AT THE JOHN E. AMOS POWER PLANT, WEST VIRGINIA

**Steven R. Hanna**
**Air Resources**
**Atmospheric Turbulence and Diffusion Laboratory**
**National Oceanic and Atmospheric Administration**
**Oak Ridge, Tennessee 37830**

## 1. INTRODUCTION

There is much current interest in cooling tower plume rise because of its importance in determining the environmental impact of cooling towers at planned power plants and industrial facilities. Some of the possible environmental problems related to heat and water emissions from cooling towers are drift deposition, ground level fog, cloud formation, and precipitation enhancement (see the conference proceedings Cooling Tower Environment - 1974.) An important factor in all of these problems is the calculation of the plume trajectory, which is often complicated by the presence of multiple sources and water phase changes in the plume. As Briggs (1975) shows, the latent heat does not strongly influence plume rise if there is no cloud present at the top of the plume. His simple formulas for plume rise can be expected to work quite well on most days for cooling tower plumes. However, if a cloud forms at the top of the plume, the final cloud height will depend partly on cloud physics process. A one dimensional plume and cloud growth model was developed to study these effects (Hanna, 1976). In this paper, the predictions of the model are compared with observations of cooling tower plume rise at the John E. Amos, W. Va. power plant (2900 MWe), reported by Kramer, et al. (1975).

## 2. PLUME AND CLOUD GROWTH MODEL

The numerical model uses Weinstein's (1970) one-dimensional cloud growth model as a basis but alters its entrainment assumption so that it agrees with known relations for the rise of buoyant stack plumes (Briggs, 1975). The cloud microphysics processes are parameterized using suggestions by Kessler (1969). Current measurements by Norman, et al. (1975) at the Keystone cooling towers and Woffinden, et al. (1976) at the Chalk Point cooling tower should help determine whether Kessler's parameterizations are valid for cloud physics processes in cooling tower clouds.

A detailed description of the model would be too lengthy to include in this short summary, but is given elsewhere (see Hanna, 1976) in a form such that it can be studied or used by others. The computer program is operational (e.g., it is being used at Argonne National Laboratory by A. Policastro) and copies of the program and its description can be obtained by writing the present author.

ATDL Contribution File No. 77/1

There are four aspects of this model that can be regarded as improvements over previous versions. First, it incorporates Briggs' (1975) suggestion that the ratio of the total effective momentum flux to the momentum flux within the plume boundary approaches 2.25, due to the fact that the ambient air above the rising plume is also accelerating. Second, based on determinations of visible plume length by Slawson, et al. (1974), and Meyer, et al. (1974), it is assumed that saturation occurs in the plume when the excess water vapor content is greater than 50% of the saturation deficit in the ambient air. Third, the effects of ambient wind speed shears are included in the equation for continuity of plume volume flux. Finally, an arbitrary assumption is made to account for the merging of multiple plumes: when the plume radius grows to one-half of the distance between the towers, the cross sectional area of the model plume increases so that it is equal to the sum of the previous areas of all the plumes.

## 3. MODEL INPUTS

During the winter of 1974-1975, Smith-Singer Meteorologists, Inc. flew a light aircraft around the three cooling tower plumes at the John E. Amos, W. Va. Power Plant (see Kramer, et al., 1975). Vertical profiles of ambient temperature, dew-point, and wind speed to heights of about 1500m were obtained, and photographs of the plume were taken. Runs were purposely made on cold, humid days when a long visible plume was expected. In all the runs analyzed in this paper, the plume was visible through its point of leveling-off, so that plume rise could easily be estimated. Consequently, all of the information needed for input to the plume and cloud growth model was available.

The three natural draft cooling towers are in a line, 200m apart. Two have a height of 132m, top radius, $R_o$, of 29m, initial vertical speed, $w_o$, of 4.6 m/s, and are each capable of servicing a generator of 800 MWe. The third tower has a height of 150m, top radius of 40m, initial vertical speed of 4.2 m/s, and is capable of servicing a generator of 1300 MWe. For this study, the plume from the third tower is modeled initially. When its radius equals 100m, it is assumed that the plumes merge and the radius automatically increases by a factor of 1.5. The plume is assumed to be initially saturated, and initial cloud and rainwater concentrations are arbitrarily assumed to be 1 g/kg. The optimum initial plume temperature $T'_{po}$ is calculated

from the manufacturer's specifications discussed by Kramer, et al. (1975):

$$T'_{po} = (297.4 + .635\ (T_d - 273))\ (1 + .01\ (1 - RH)) \qquad (1)$$

where $T_d$ and RH are ambient dewpoint and relative humidity, and temperatures have the units °K. To account for differences in plant load, the following relation is used to calculate the actual initial plume temperature:

$$T_{po} - T_{eo} = C \cdot (T'_{po} - T_{eo}) \qquad (2)$$

where $T_{eo}$ is the ambient temperature at tower top and C is the ratio of actual plant load to full load (2900 MWe). For bent over plumes (wind speed, U, less than 1 m/s), an effective initial plume radius, $R_{eff}$, is used in order to maintain continuity of the momentum flux (Hanna, 1972):

$$R_{eff} = R_o\ (w_o/U)^{1/2} \qquad (3)$$

## 4. RESULTS

Input conditions for three typical runs are given in Table 1. These input data and results are given in detail so that they can be used by others for model comparison.

TABLE 1

Input conditions for runs 1, 10, and 15. Height z refers to height above tower top

| | Run 1 | | | Run 10 | | | Run 15 | | |
|---|---|---|---|---|---|---|---|---|---|
| z(m) | $T_e$(°K) | $T_d$(°K) | U($\frac{m}{s}$) | $T_e$(°K) | $T_d$(°K) | U($\frac{m}{s}$) | $T_e$(°K) | $T_d$(°K) | U($\frac{m}{s}$) |
| 0 | 268.6 | 264.2 | 13.5 | 268.0 | 264.7 | 2.2 | 261.3 | 261.3 | 0 |
| 91 | 267.4 | 264.1 | 13.5 | 267.5 | 264.2 | 4.9 | 265.7 | 259.6 | 0 |
| 213 | 269.1 | 262.4 | 13.5 | 266.3 | 264.1 | 4.9 | 265.2 | 258.5 | 0 |
| 304 | 269.1 | 260.0 | 13.5 | 265.2 | 263.5 | 4.9 | 267.7 | 257.4 | 0 |
| 456 | 269.1 | 257.4 | 13.5 | 264.1 | 263.0 | 4.9 | 265.2 | 256.3 | 0 |
| 578 | 270.2 | 245.2 | 16. | 263.0 | 262.5 | 6.7 | 264.7 | 254.6 | 2.5 |
| 669 | 270.8 | 247.5 | 16. | 262.5 | 262.5 | 8.9 | 264.7 | 249.7 | 5.5 |
| 821 | 271.3 | 252.4 | 16. | 264.7 | 256.4 | 8.9 | 264.7 | 249.7 | 5.5 |
| 942 | 272.4 | 254.1 | 16. | 265.8 | 251.9 | 8.9 | 264.1 | 247.4 | 5.5 |
| 1064 | 271.3 | 259.1 | 16. | 266.9 | 248.6 | 8.9 | 263.0 | 246.9 | 6.0 |
| | C = .98 | | | C = .98 | | | C = .98 | | |
| | $T_{po}$ = 292.3 | | | $T_{po}$ = 292.6 | | | $T_{po}$ = 289.4 | | |
| | Observed Rise = 560m | | | Observed Rise = 820m | | | Observed Rise = 1120m | | |

The predicted profiles of vertical speed, w, plume-ambient temperature difference, $(T_p - T_e)$, and cloud water content, $Q_c$, for these three runs are plotted in Figures 1 through 3.

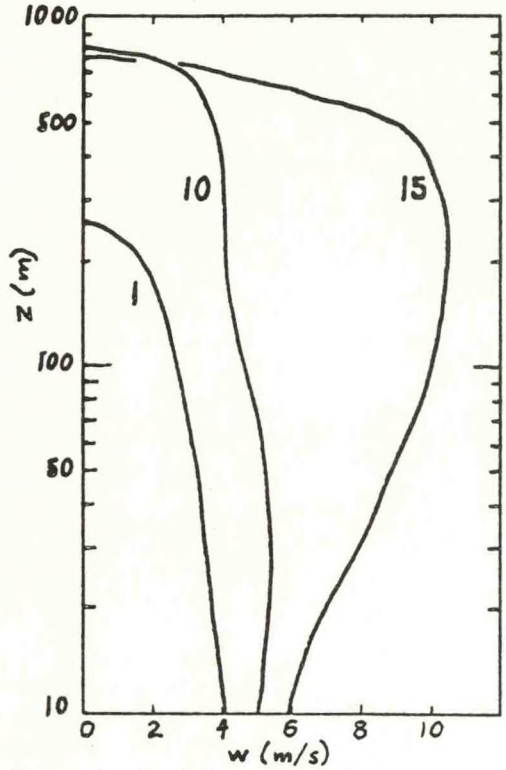


Figure 1: Variation of calculated vertical speed, w, with height for runs 1, 10, and 15.

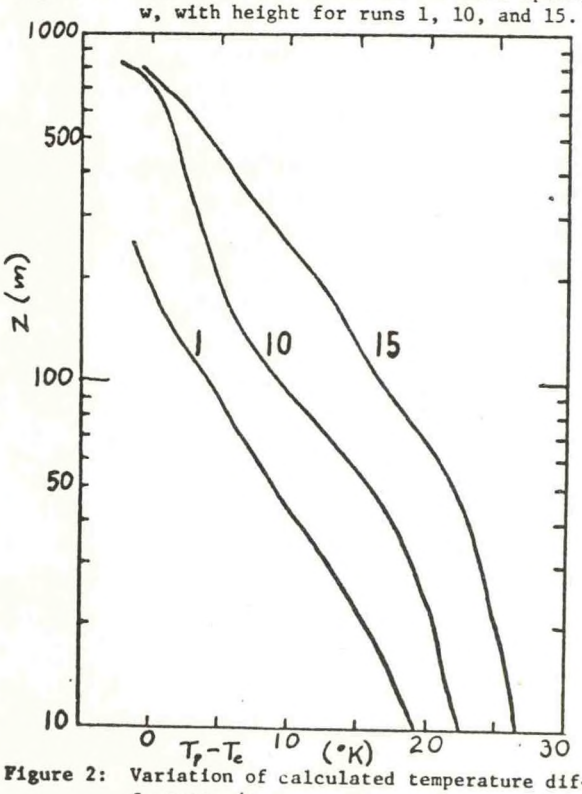


Figure 2: Variation of calculated temperature difference, $(T_p - T_e)$ with height for runs 1, 10, and 15.

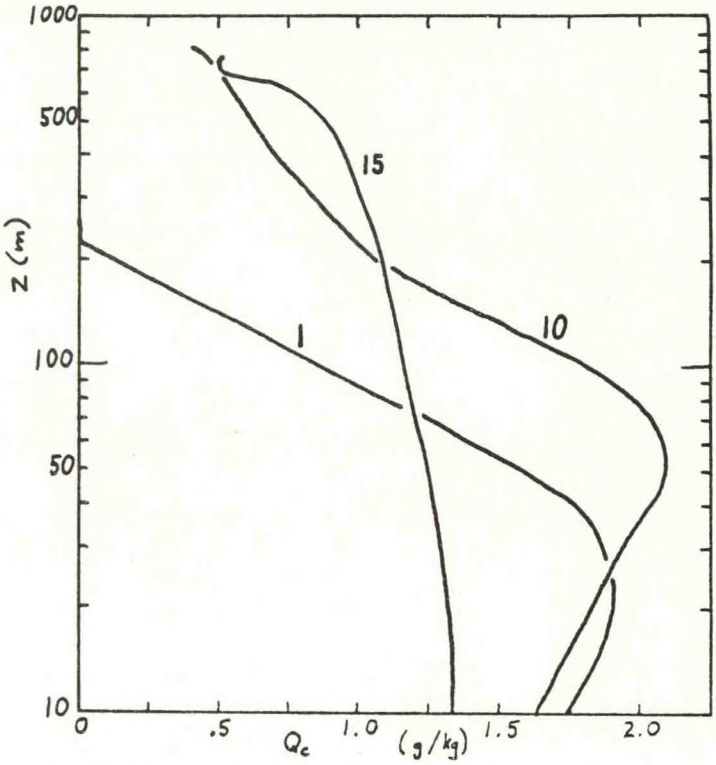


Figure 3: Variation of calculated cloud water content, $Q_c$, with height for runs 1, 10, and 15.

Runs 1 and 10 are bent over plumes and run 15 is a vertical plume which bends over above a height of about 600m. Because of the reduced entrainment rate for the vertical plume, its temperature difference and vertical speed do not decrease with height as fast as those for the bent over plumes. However, because the ambient air is drier for the vertical plume than for the two bent over plumes, the cloud water content $Q_c$ of the vertical plume is not much different from that of the bent over plumes. As the wind speed increases above 1 m/s at a height of about 500 m in run 15, the entrainment coefficients switch from those applying to a vertical plume to those applying to a bent over plume. The visible plume in run 1 is predicted to evaporate just below the height of final plume rise, while the observed visible plume on that day extended through the height of maximum plume rise. Cloud water content at the top of the plumes in runs 10 and 15 is about .5 g/kg, a value within the range of measured cloud water content in natural clouds. Measurements of the cloud water content of the plume during these runs would have been useful, but unfortunately in-plume measurements were not part of this program.

The plumes in the bent over runs are predicted to merge at a height of about 200m, in agreement with the observations. The plumes in run 15 do not merge until a height of about 500m is reached due to the reduced entrainment. This is also in rough

agreement with observations, although the prediction of a constriction in the plumes just above the tower top for vertical plumes is not verified by the Amos photographs.

A summary of observed and predicted plume rise for all of the runs analyzed in this program is given in Table 2.

TABLE 2

Observed and Calculated Plume Rise

| Run | $\bar{U}_{(m/s)}$ | Inversion height above tower (m) | Observed plume rise (m) | Model plume rise (m) | Analytical plume rise, sensible, one unit (m) |
|---|---|---|---|---|---|
| 1 | 14 | | 560 | 260 | 250 |
| 6 | 11 | | 850 | 820 | 430 |
| 8 | 9 | | 370 | 350 | 250 |
| 10 | 6 | 720 | 820 | 820 | 590 |
| 11 | 0 | 660 | 880 | 900 | 980 |
| 12 | 6 | 1140 | 1060 | 1200 | 720 |
| 15 | 3 | | 1120 | 790 | 780 |
| 16 | 6 | 1200 | 1160 | 700 | 380 |
| 17 | 8 | 360 | 360 | 430 | 410 |
| 18 | 6 | | 910 | 720 | 410 |
| 19 | 0 | 840 | 800 | 970 | 910 |
| 24 | 6 | 750 | 760 | 630 | 500 |
| 28 | 5 | | 360 | 400 | 310 |
| 31 | 0 | | 500 | 900 | 780 |
| 35 | 3 | 390 | 360 | 590 | 480 |
| 44 | 8 | 960 | 910 | 420 | 510 |
| 45 | 7 | 1200 | 910 | 370 | 390 |
| 47 | 0 | 900 | 800 | 1020 | 910 |
| 48 | 7 | 750 | 670 | 360 | 340 |
| Avg. | 5.6 | 820 | 750 | 670 | 540 |

The average model and observed plume rises are 670m and 750m, respectively, and the correlation coefficient is 0.49. It can be concluded that the plume and cloud growth model can be satisfactorily used to estimate the plume characteristics and the development of clouds due to cooling tower emissions.

The plume rise predicted by Briggs' (1975) well-known analytical formulas is included in the last column of Table 2. In the application of this formula, the initial buoyancy flux is assumed to equal the sensible heat flux from the largest tower. It is seen that the average predicted plume rise is 540m and the correlation with observations is .37.

The height of the base of the capping inversion or the "mixing layer" is also listed in Table 2. Brennan, et al.(1976) have analyzed these data and find that, when a capping inversion is present, the plume will generally rise to this height and level off. For the data in Table 2 the correlation between capping inversion height and observed plume rise is 0.90. A good general rule might be that, when an inversion caps a mixed layer, and the base of this inversion is at a height of less than about 1 km, then the final plume rise from cooling towers as large as those at the Amos plant will equal the inversion height. By the nature of the Amos experiments (cold winter mornings) low mixing heights could be expected. But during other seasons of the year the mixing heights will increase and it will be much less likely that the plume will reach the capping inversion.

Acknowledgements. The cooperation of Smith-Singer Meteorologists, Inc. and the American Electric Power Service Corporation in providing the Amos data is greatly appreciated. This work was performed under an agreement between the National Oceanic and Atmospheric Administration and the Energy Research and Development Administration.

## References

Brennan, P. T., D. E. Seymour, M. J. Butler, M. L. Kramer, M. E. Smith and T. T. Frankenburg, 1976: The observed rise of visible plumes from hyperbolic natural draft cooling towers. Atmos. Environ., in press.

Briggs, G. A., 1975: Plume rise predictions. Lectures on Air Pollution and Environmental Impact Analyses. American Meteorol. Soc., 45 Beacon St., Boston, Mass., 59-111.

Cooling Tower Environment - 1974, ERDA Symposium Series, CONF-740302, Nat. Tech. Information Service, U.S. Dept. of Commerce, Springfield, Va., 22161, ($13.60), 638 pp.

Hanna, S. R., 1972: Rise and condensation of large cooling tower plumes. J. Appl. Meteorol., 11, 793-799.

Hanna, S. R., 1976: Predicted and observed cooling tower plume rise and visible plume length at the John E. Amos power plant. To be published in Atmos. Environ., available as No. 75/25 from ATDL, P. O. Box E, Oak Ridge, Tn. 37830; 39 pp plus 5 figures.

Kessler, E., 1969: On the distribution and continuity of water substance in atmospheric circulations. Meteorol. Monographs, 10, 84 + ixpp, published by the Amer. Meteorol. Soc., 45 Beacon St., Boston.

Kramer, M. L., D. E. Seymour, M. J. Butler, R. N. Kempton, P. J. Brennan, J. J. Conte and R. G. Thomson, 1975: John E.Amos Cooling Tower Flight Program Data, December 1974-March 1975. Smith-Singer Meteorologists, Inc., 134 Broadway, Amityville, N. Y. 11701 for American Electric Power Service Corp., P. O. Box 487, Canton, Ohio 44701.

Meyer, J. H., T. W. Eagles, L. C. Kohlenstein, J. A. Kagan and W. D. Stanbro, 1974: Mechanical draft cooling tower visible plume behavior: Measurements, models, predictions. In Cooling Tower Environment - 1974, ERDA Symposium Series, CONF-740302, pp 307-352.

Norman, J. M., D. W. Thomson, J. Pena and R. Miller, 1975: Aircraft turbulence and drift water measurements in evaporative cooling tower plumes. Dept. of Meteor., Penn. State Univ., University Park, Pa. 16802.

Slawson, P. R., J. H. Coleman and J. W. Frey, 1974: Some observations on cooling-tower plume behavior at the Paradise Steam Plant. In Cooling Tower Environment - 1974, ERDA Symposium Series, CONF-740302, pp 147-160.

Weinstein, A. I., 1970: A numerical model of cumulus dynamics and microphysics. J. Atmos. Sci., 27, 246-255.

Woffinden, G. J., J. A. Anderson and P. R. Harrison, 1976: Aircraft Survey, Chalk Point Cooling Tower Plume, Dec. 1975. Rep. No. 76R-1410 by MRI, Altadena, Cal. 91001 for the Maryland Power Plant Siting Program, 33 pp + appendices.